Search for a spin-zero particle in Higgs boson decays or top-associated production using the ATLAS detector

Paula Martínez Suárez

Ph. D. defence, 11 March 2025

Thesis supervisor: *Imma Riu Dachs*
Thesis tutor: *José María Crespo Vicente*

Overview

- Introduction
- Theoretical framework
- Experimental setup
- Physics simulation
- $H \rightarrow aa \rightarrow 4b$ search
- tta, $a \rightarrow bb$ search
- Summary

Introduction

- The Standard Model is the **most successful** theory for describing Physics at the **fundamental level**.
- However, on its own, it **can not explain** everything that we observe in the universe.
- This thesis explores the existence of **new light pseudoscalar particles**.
  - If they couple to the SM Higgs boson $\Rightarrow$ *exotic Higgs decays?* $\mathbf{BR}(H \to \mathbf{undetected}) \lesssim 12\%$
  - If they couple strongly to heavy fermions $\Rightarrow$ *top-associated production?*

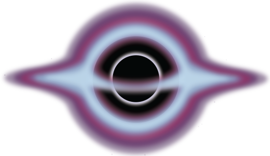

Theoretical framework

The Standard Model of Particle Physics

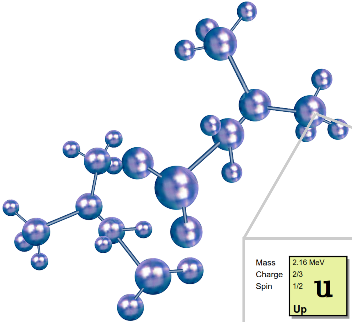

The **Standard Model** describes all fundamental particles and their interactions (*except gravity*). Is is a quantum field theory based on the $\mathbf{SU(3)_C \times SU(2)_L \times U(1)_Y}$ gauge symmetry group.

Mass / Charge / Spin

Quarks	2.16 MeV, 2/3, 1/2, **u** Up	1.2730 GeV, 2/3, 1/2, **c** Charm	172.57 GeV, 2/3, 1/2, **t** Top	0, 0, 1, **g** Gluon	125.20 GeV, 0, 0, **H** Higgs	
Quarks	4.70 MeV, -1/3, 1/2, **d** Down	93.5 MeV, -1/3, 1/2, **s** Strange	4.183 GeV, -1/3, 1/2, **b** Bottom	0, 0, 1, **γ** Photon		
Leptons	0.5110 MeV, -1, 1/2, **e** Electron	105.6584 MeV, -1, 1/2, **μ** Muon	1776.93 MeV, -1, 1/2, **τ** Tau	91.1880 GeV, 0, 1, **Z** Z boson		Gauge bosons
Leptons	~ 0, 0, 1/2, ν_e e neutrino	~ 0, 0, 1/2, ν_μ μ neutrino	~ 0, 0, 1/2, ν_τ τ neutrino	80.3692 GeV, ±1, 1, **W** W boson		Gauge bosons

- Quarks and leptons (spin-1/2) are the constituents of matter.
- Gauge bosons (spin-1) are the force carriers.
  - $g \leftrightarrow$ strong force.
  - $\gamma \leftrightarrow$ electromagnetic force.
  - $Z, W^{\pm} \leftrightarrow$ weak force.
- The Higgs boson (spin-0) gives mass to particles via the **Higgs mechanism**.

The Brout-Englert-Higgs mechanism

- Conventional mass terms in the SM lagrangian do not respect the $\mathbf{SU(2)_L \times U(1)_Y}$ symmetry.
- The Higgs field causes the spontaneous symmetry breaking $\mathbf{SU(2)_L \times U(1)_Y \rightarrow U(1)_{EM}}$.
- In this process, the **Z and $W^{\pm}$ bosons** acquire their masses, consistent with experimental observations.

Fermions acquire mass terms through their interaction with the Higgs boson:

$$\mathcal{L}_{\text{Yukawa}} \ni -\underbrace{\frac{\lambda_f v}{\sqrt{2}}}_{m_f} \bar{f} f - \underbrace{\frac{\lambda_f}{\sqrt{2}}}_{m_f/v} \bar{f} f\, H$$

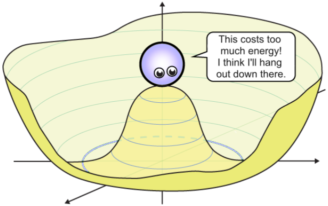

$$V(\Phi) = -\mu^2 (\Phi^\dagger \Phi) - \lambda (\Phi^\dagger \Phi)^2$$

$$\langle \Phi \rangle = \frac{1}{\sqrt{2}} \begin{pmatrix} 0 \\ v \end{pmatrix} \xrightarrow[\text{around the vacuum}]{\text{Oscillations}} \frac{1}{\sqrt{2}} \begin{pmatrix} 0 \\ v + H \end{pmatrix}$$

Beyond the Standard Model

The SM has successfully predicted with high precision decades of discoveries in the field of Particle Physics.

However, it can not explain...

- The Higgs hierarchy problem.
- The values of particle masses.
- The strong CP problem.

And also...

- Dark matter and dark energy.
- The matter-antimatter asymmetry.
- Neutrino masses.
- The muon $(g-2)$ anomaly.

Is there Physics beyond the Standard Model?

This thesis explores extensions of the SM featuring axion-like particles (ALPs).

- Pseudoscalar particles.
- Can be light w.r.t. the EW energy scale.
- Can inherit Yukawa-like couplings from the SM Higgs boson.

Slides 54 – 56.

Experimental setup

The ATLAS experiment at the LHC

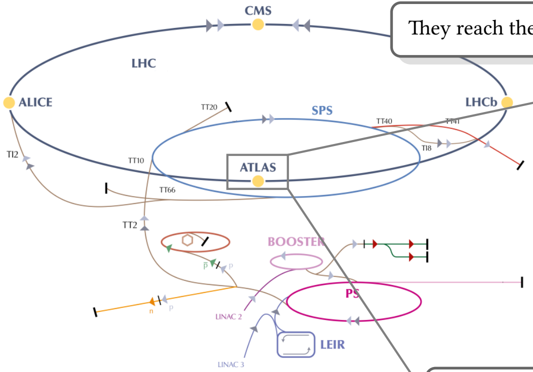

They reach their maximum energy at the **LHC** ring, which is 27 km long.

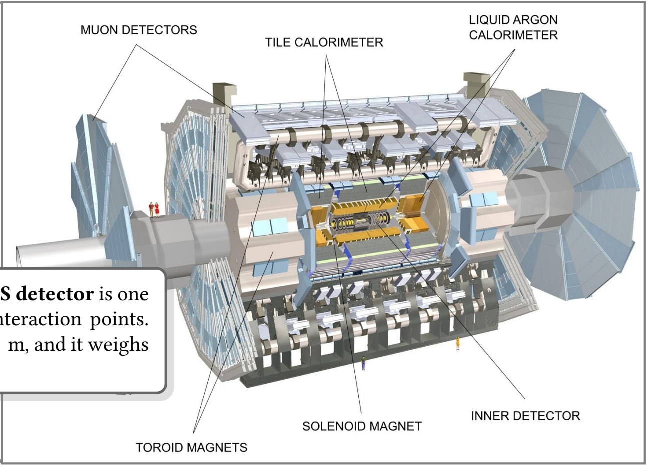

Protons are extracted from hydrogen atoms and accelerated in bunches through a series of machines.

The **ATLAS detector** is one of the 4 interaction points. It is 46×25 m, and it weighs 7000 T.

Inner detector (ID)

Slide 58.

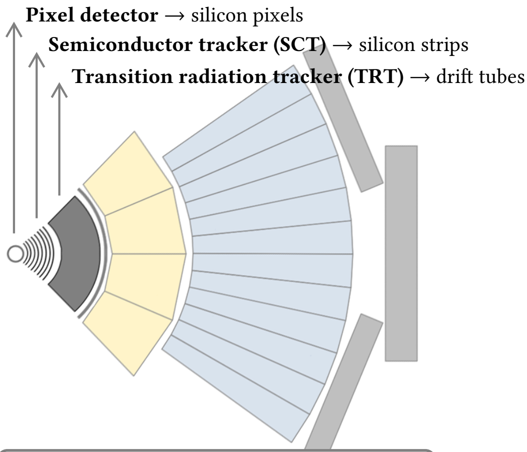

The **ID** is the first point of detection, located just **a few cm** away from the collision point.

Charged particles leave **tracks** in the ID. Using pattern recognition algorithms, they are matched to their corresponding interaction **vertices**.

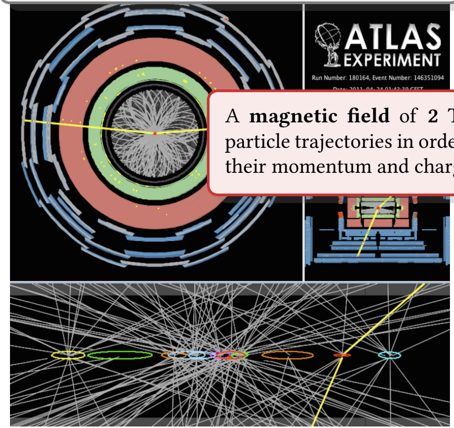

A **magnetic field** of **2 T** bends the particle trajectories in order to identify their momentum and charge.

Liquid argon (LAr) calorimeter

Slide 59.

The **LAr calorimeter** uses plates of **absorber material** to trigger particle cascades that ionise the **active material**, producing a measurable signal.

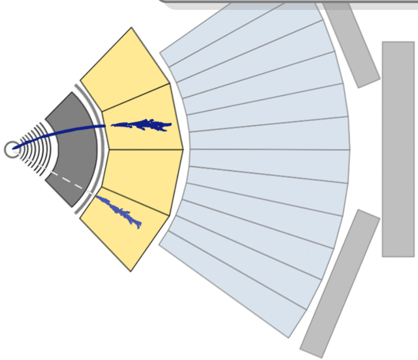

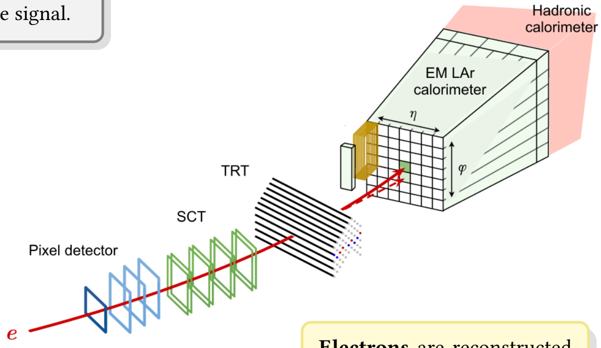

Electrons are reconstructed from **energy deposits** in the LAr calorimeter associated to ID **tracks**.

Absorber material: lead or copper.
Active material: liquid argon.

Tile calorimeter (TileCal)

The **TileCal** uses steel plates as the **absorber material** and tiles of plastic scintillators as the **active material**.

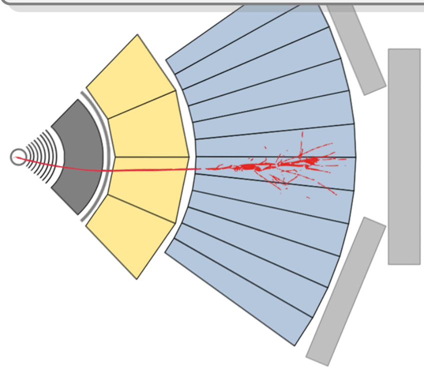

Hadrons interact with the material producing particle cascades (**jets**) and leaving **energy deposits** in the tile calorimeter.

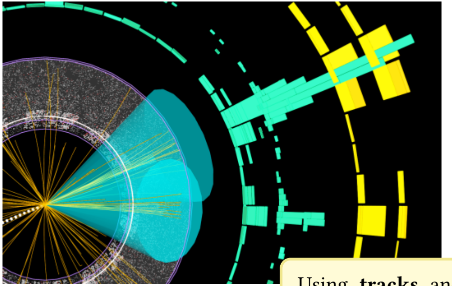

Using **tracks** and **calorimeter** information, jets are **clustered** into **cones** of fixed radius.

Slides 59, 60.

Muon spectrometer (MS)

Slide 61.

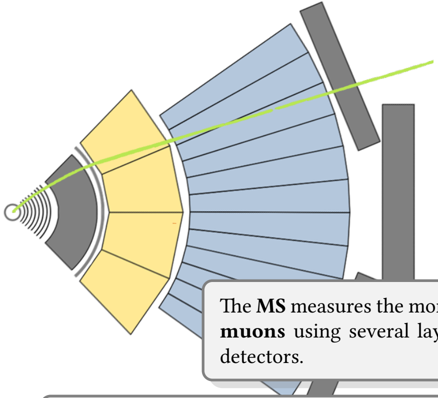

Muons are reconstructed from **tracks**, **TileCal** and **MS** information.

The **MS** measures the momentum of **muons** using several layers of gas detectors.

When a muon passes through the detector, it **ionises** the gas, triggering an **electric signal** that can be recorded by the different sensors.

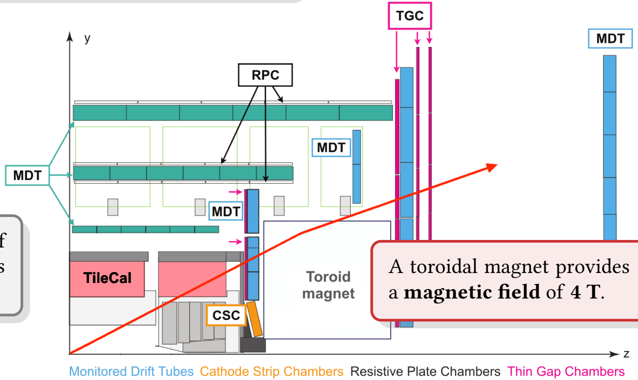

A toroidal magnet provides a **magnetic field** of **4 T**.

Invisible particles?

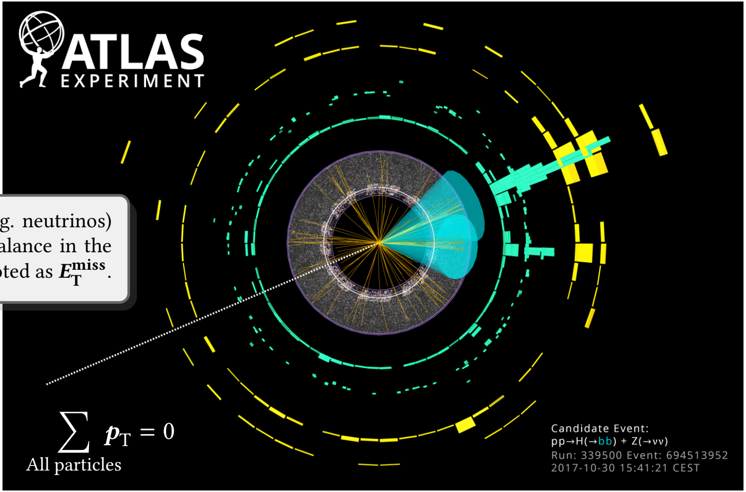

Invisible particles (e. g. neutrinos) cause an energy imbalance in the transverse plane denoted as E_T^{miss}.

$$\sum_{\text{All particles}} p_T = 0$$

Trigger and data acquisition

Slides 62, 63.

The **Level-1 trigger** is a `hardware-based` system that works with **partial** detector granularity. It has a latency of **∼2.5 μs**.

Level-1 trigger
Input rate: 40 Mhz
Output rate: 100 kHz

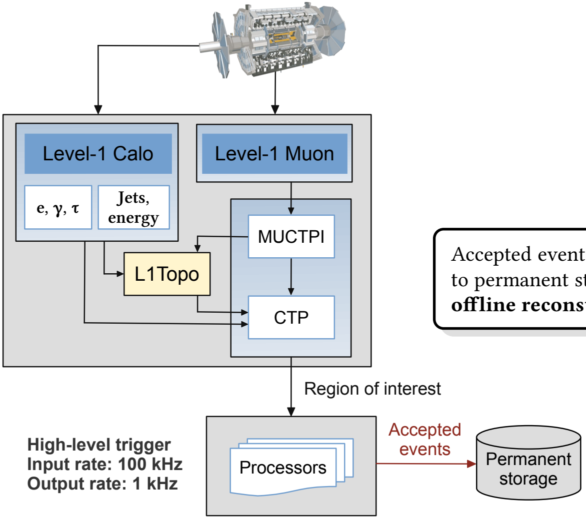

Accepted events are sent to permanent storage for **offline reconstruction**.

The **HLT** is a `software-based` trigger that reconstructs the event with **full** detector granularity. It has a latency of **∼200 ms**.

Physics simulation

Anatomy of an ATLAS event

Hard scattering: the main interaction between two partons from the proton bunches.

Parton shower: soft and collinear QCD emissions originating from the initial- and final-state particles.

Hadronisation and decay: it occurs due to the colour confinement of non-perturbative QCD at low energies.

EM radiation.

Underlying event: additional particle interactions that do not originate from the hard scattering.

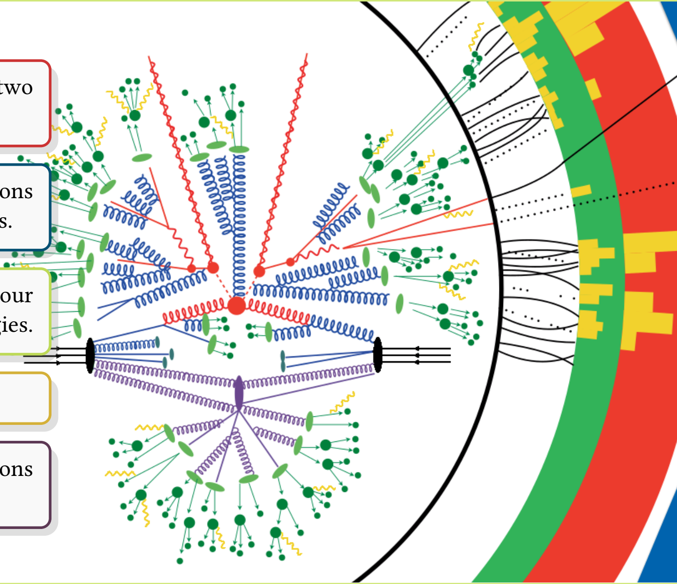

Slide 65.

Search for decays of the Higgs boson into pseudoscalar particles decaying to four bottom quarks using proton-proton collisions at $\sqrt{s} = 13$ TeV with the ATLAS detector

Motivation

Search for a new light pseudoscalar (a) produced in **Higgs boson** decays in the **4*b*** final state using a simplified model approach:

$$\mathcal{L} \ni \underbrace{\frac{1}{2}(\partial_\mu a)(\partial^\mu a)}_{\text{Kinetic term}} - \underbrace{\frac{1}{2}m_a^2 a^2}_{\text{Mass term}} - \underbrace{\frac{1}{2}\lambda_a a^2 H}_{\text{Coupling to } H} - \underbrace{y_b a \bar{b}(i\gamma^5) b}_{\text{Coupling to } b}$$

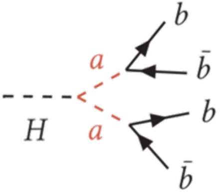

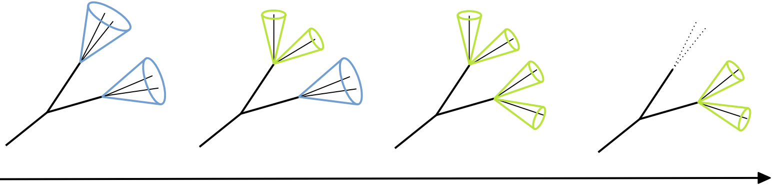

Boosted decays
(Low m_a)

Resolved decays
(High m_a)

$\boldsymbol{m_a} \in$ **[12, 60] GeV.**

Different a-boson masses
$\Rightarrow$ **different topologies**.

Slide 70.

A more detailed view of *b*-quark identification

Jets originating from ***b*-quarks** can be identified by their **substructure**.

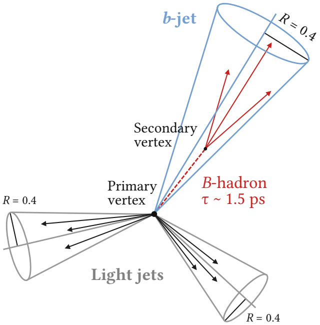

A ***b*-jet** has a radius ***R* = 0.4** and it contains a **secondary vertex** from *B*-hadron decay.

When two *b*-quarks are **very close**, they can not be reconstructed individually.

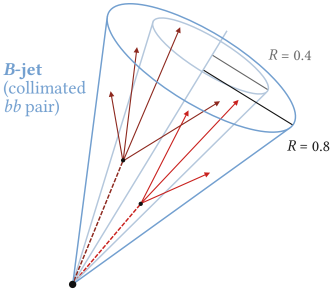

A ***B*-jet** has a radius ***R* = 0.8** and contains a **collimated $b\bar{b}$ pair**.

If the *b*-quark has **very low p_T**, it can not be reconstructed as a jet.

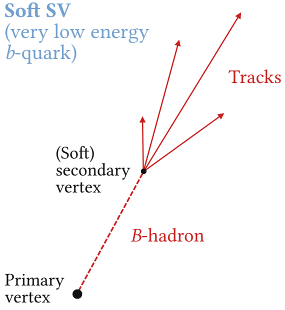

Soft SVs (ν) are reconstructed from **tracks** only.

Slides 67 – 69.

Data samples

Data samples

Full Run 2 dataset (2015-2018).

- $\int \mathcal{L} dt = 140$ fb^{-1}
- $\sqrt{s} = 13$ TeV

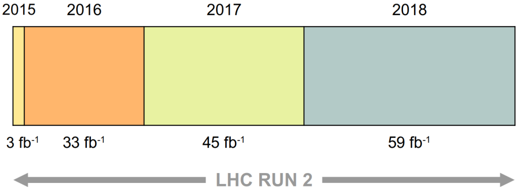

There are 2 previous ATLAS searches using **partial** Run 2 data:

Phys. Rev. D 102 (2020) 112006 (15-30 GeV)
JHEP 10 (2018) 031 (20-60 GeV)

Monte Carlo samples

Signal samples

- ZH production at tree-level and 1-loop.
- $Z \to \ell\ell$ final state.
- $m_H = 125$ GeV.
- $\mathrm{BR}(H \to aa \to 4b) = 1$.
- 8 mass hypotheses:
  $\boldsymbol{m_a \in [12, 16, 20, 25, 30, 40, 50, 60]}$ **GeV**.

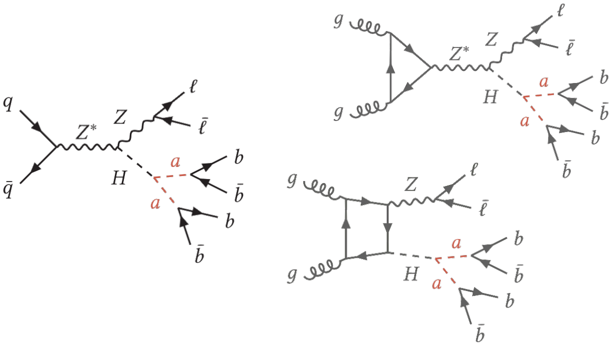

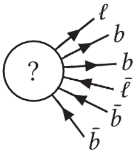

Background samples

Top backgrounds: $t\bar{t}$+jets, single-top, $t\bar{t}H$, $t\bar{t}Z$, $t\bar{t}W$, tZ, tWZ.

Vector-boson backgrounds: Z+jets, W+jets, ZZ, ZW, WW.

Event selection (preselection)

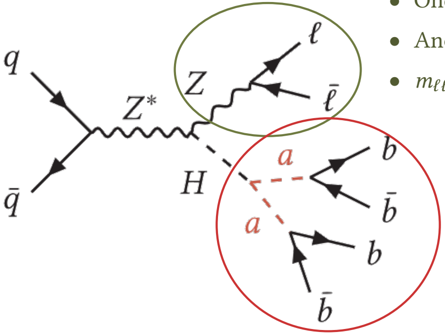

$Z \to \ell\ell$ selection

- 2 leptons ($\boldsymbol{ee}$, $\boldsymbol{\mu\mu}$ or $\boldsymbol{e\mu}$).
- One **trigger** lepton with $p_{\mathrm{T}} > 27$ GeV.
- Another lepton with $p_{\mathrm{T}} > 10$ GeV.
- $m_{\ell\ell} > 50$ GeV.

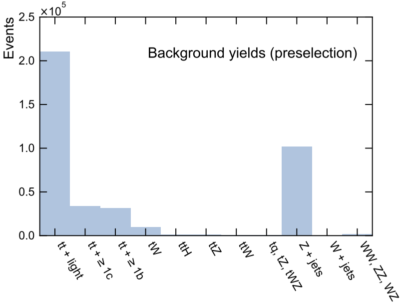

b selection

- $(2N_B + N_b + N_v) \geq 3$

Background modelling

- The **two main backgrounds** are $t\bar{t}$+jets and Z+jets.
- Mismodelling observed in both normalisation and shape.
- **Data-driven** corrections (reweighting) calculated in **signal-depleted regions**.

tt+jets reweighting region

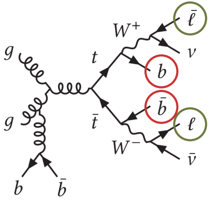

- Preselection
- $e\mu$ with $|m_{e\mu} - m_Z| < 20$ GeV
- $N_b \geq 2$

Z+jets reweighting region

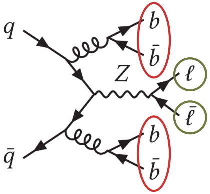

- Preselection
- ee or $\mu\mu$ with $|m_{\ell\ell} - m_Z| < 20$ GeV
- $(2N_B + N_b + N_\nu) = 3$
- $E_T^{miss} < 60$ GeV

Normalisation correction

The normalisation of $t\bar{t}$+light, $t\bar{t}+\geq 1c$ and $t\bar{t}+\geq 1b$ is corrected using a fit to the `sumPCBTag` distribution:

$$\texttt{sumPCBTag} = \sum \text{PC } b\text{-tagging score}^{*} \text{ of all jets}$$

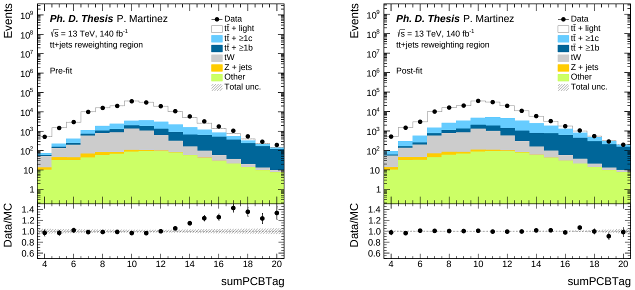

This is not necessary for the Z+jets Monte Carlo sample.

* The ***b*-tagging score** is a value between 1 and 5 assigned to each jet, representing the **likelihood** that it originates from a *b*-quark:

1 – Not likely.

5 – Very likely.

N_{jets} shape correction

$t\bar{t}$+jets RW

Z+jets RW

Shape mismodelling in the $\boldsymbol{N_{jets}}$ distribution corrected by adjusting **each bin** to data.

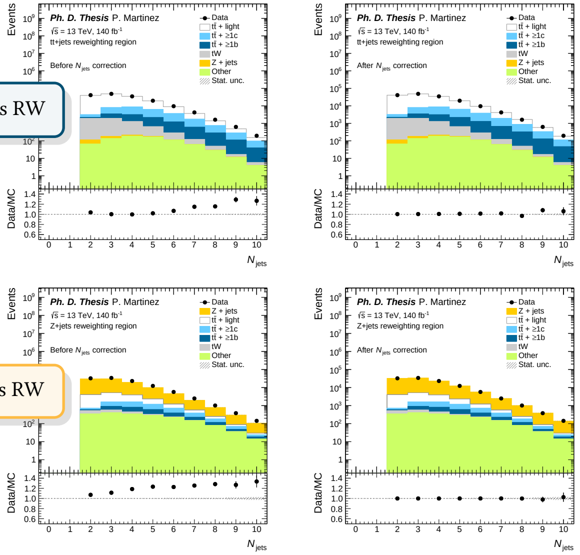

p_T shape correction

- Residual shape mismodelling in jet and lepton $\boldsymbol{p_T}$.
- For $t\bar{t}$+jets, corrected using $H_T = \sum(p_T^{\text{jets}} + p_T^{\text{lep}})$.
- **Strong correlation** between H_T and N_{jets}
  $\Rightarrow$ using $H_T^{\text{red}} = H_T - (N_{\text{jets}} - 2)\Delta H_T$.

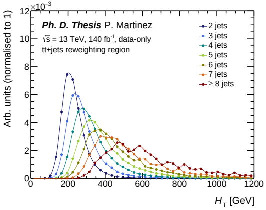

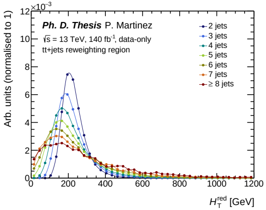

- For Z+jets, the $\boldsymbol{Z}$ **boson's** $\boldsymbol{p_T}$ is used instead.

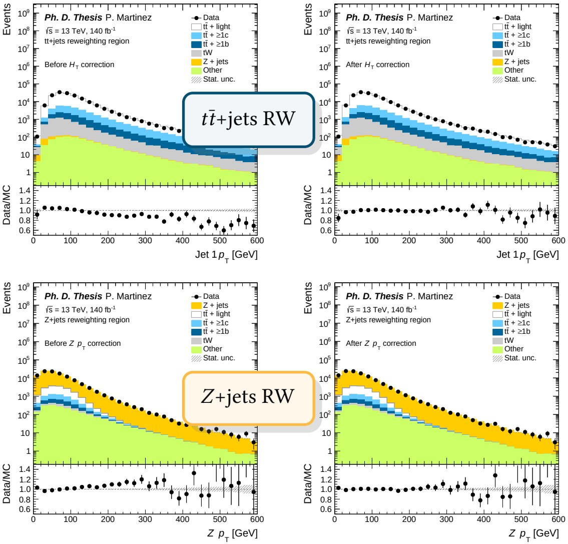

Slides 71 – 73.

NN for event reconstruction

- **Mass-parametrised** neural network.
- Used to find the **best object pairing** in the **4*b* final state**.
- **5 hypotheses** are considered: 2B, 1B2b, 1B1b1v, 4b, 3b1v.

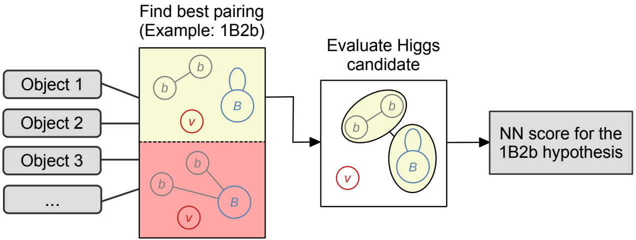

- The **preferred hypothesis** is the one with the **highest score**.
- This hypothesis is used to **reconstruct** the *a* and Higgs boson.

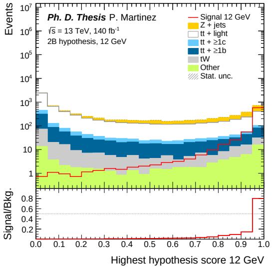

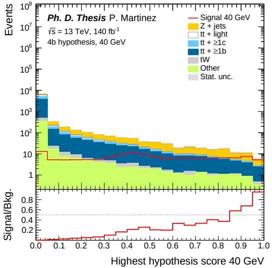

Slide 74.

BDT for signal vs. background discrimination

- One boosted decision tree **for each** NN hypothesis and *a*-boson mass.
- Inputs include:
  - Reconstructed ***a*- and *H*-boson** variables from the NN.
  - ***Z*-boson** ($\ell\ell$ pair) kinematics.
- The **BDT score** is classified in **3 bins** according to their signal content: Loose, Medium and Tight.

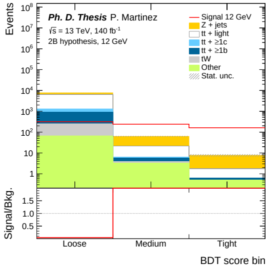

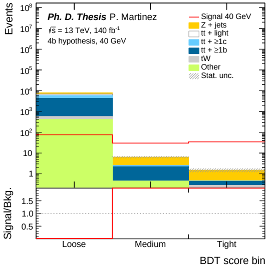

Slide 75.

Signal and control regions

Signal regions

NN hypothesis + additional cuts

- 2B
- 1B2b
- 1B1b1v
- 4b
- 3b1v

ee or $\mu\mu$
$|m_{\ell\ell} - m_Z| \leq 20$ GeV
High NN score

Control regions

b-object count + additional cuts

- $2B$ (Loose B-tagging)
- $2B$ (Tight B-tagging)
- $1B + 2b$ (Loose B-tagging)
- $1B + 2b$ (Tight B-tagging)
- $4b$
- $3b$ + $1v$ or 1 jet

Z+jets selection
ee or $\mu\mu$
$|m_{\ell\ell} - m_Z| \leq 10$ GeV
Low NN score
$E_T^{miss} < 60$ GeV

$t\bar{t}$+jets selection
$e\mu$

Slide 76.

Systematic uncertainties

Experimental uncertainties

Detector response, efficiency and calibration. Applied to all signal and background processes.

- Luminosity.
- Pileup modelling.
- Trigger efficiency.
- Object reconstruction and identification (electrons, muons, jets and tracks).
- Flavour tagging.
- $E_{\mathrm{T}}^{\mathrm{miss}}$.

Modelling uncertainties

Theoretical assumptions and limitations in the MC simulation. Applied to signal and the main backgrounds ($t\bar{t}$+jets and Z+jets).

- Renormalisation and factorisation scales (μ_{R}, μ_{F}).
- Parton distribution functions (PDFs).
- Initial and final state radiation (ISR and FSR).
- Alternative hard scattering simulation.
- Alternative parton shower simulation.
- Reweighting uncertainties.

Fit setup

Statistical treatment

- One fit per mass hypothesis (8 in total):
  $\boldsymbol{m_a} \in$ **[12, 16, 20, 25, 30, 40, 50, 60] GeV**
- Binned maximum-likelihood fit to the data.

  Free parameters:
  - Signal strength (μ)
  - 3 $t\bar{t}$+jets normalisation factors
  - 1 Z+jets normalisation factor.
- Systematic uncertainties enter the fit as **nuisance parameters**.
  - Pruning at 1%.

Signal and control regions

- 5 SRs $\Rightarrow$ Fit to the **BDT bins**.

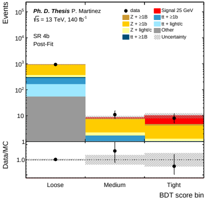

- 6 CRs for Z+jets and 6 CRs for $t\bar{t}$+jets.
  $\Rightarrow$ Fit to the **yield** per region.

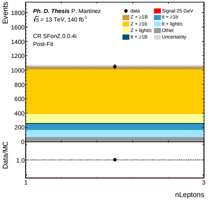

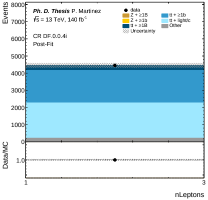

Results from the fit to data (m_a = 25 GeV)

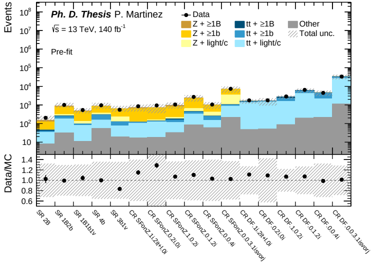

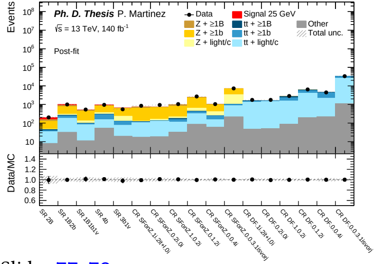

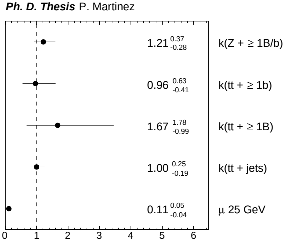

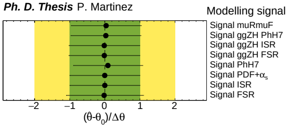

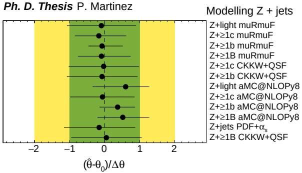

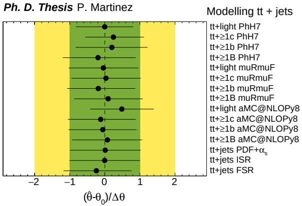

Slides 77, 78.

Exclusion limits

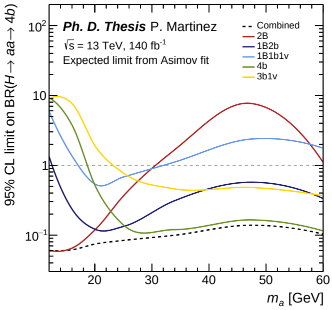

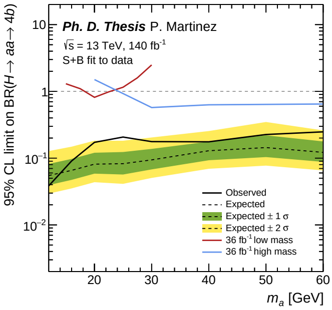

Category	Impact on $\hat{\mu}$
Total stat.	33.1%
Total syst.	22.5%
General	2.4%
Lepton reconstruction	0.3%
Jet reconstruction	7.8%
Track reconstruction	1.5%
E_T^{miss}	0.8%
Flavour tagging	11.6%
Signal modelling	8.2%
Z+jets modelling	5.4%
$t\bar{t}$+jets modelling	4.8%
Reweighting	0.7%
MC stats.	13.0%
Signal MC stats.	1.7%
Norm. factors	3.5%

- **No significant excess** above the SM is observed.
- 95% CL limits to the $\mathbf{BR(H \to aa \to 4b)}$ **between 5% and 25%** for $\boldsymbol{m_a \in [12, 60]}$ **GeV**.
- The dominant source of uncertainty is **statistics**.
- **Great improvement** w.r.t. previous analyses.

Slide 79.

Search for a new pseudoscalar decaying into a pair of bottom and anti-bottom quarks in top-associated production using proton-proton collisions at $\sqrt{s} = 13$ TeV with the ATLAS detector

Search for a new light pseudoscalar (a) produced in association with **top quarks** in the $\boldsymbol{a \to b\bar{b}}$ final state using a simplified model approach:

$$\mathcal{L} \ni \underbrace{\frac{g_t y_t}{\sqrt{2}} \bar{t}(i\gamma^5) a t}_{\text{Coupling to } t} + \underbrace{\frac{g_b y_b}{\sqrt{2}} \bar{b}(i\gamma^5) a b}_{\text{Coupling to } b}$$

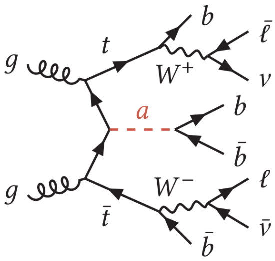

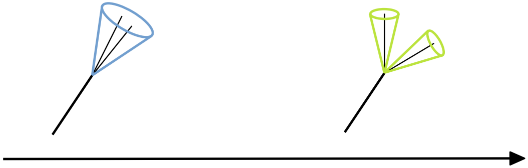

Boosted decays
(Low m_a)

Resolved decays
(High m_a)

$\boldsymbol{m_a \in [12, 100]}$ **GeV**

Low $m_a \Rightarrow$ boosted a-decay (B-jet).
High $m_a \Rightarrow$ resolved a-decay (b-jets).

Slides 81, 82.

Data samples

Full Run 2 dataset (2015-2018)

- $\int \mathcal{L} dt = 140 \text{ fb}^{-1}$
- $\sqrt{s} = 13$ TeV

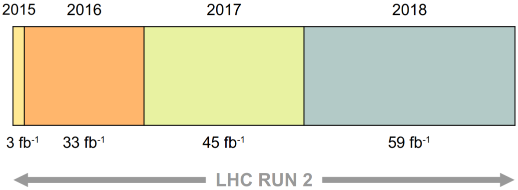

First search of its kind in ATLAS and CMS.

Monte Carlo samples

Signal samples

- $t\bar{t}a$ and tWa production.
- $t\bar{t} \to \ell\ell$ final state.
- $g_t = 0.5$.
- $\mathrm{BR}(a \to b\bar{b}) = 1$.
- 10 mass hypotheses:
  $\boldsymbol{m_a \in [12, 16, 20, 50, 30, 40, 50, 60, 80, 100]}$ **GeV**.

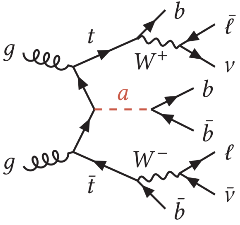

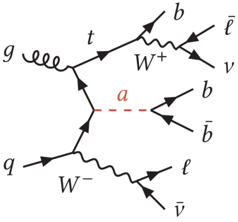

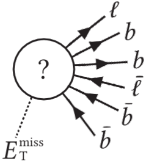

Background samples

Top backgrounds: $t\bar{t}$+jets, single-top, $t\bar{t}H$, $t\bar{t}Z$, $t\bar{t}W$, tZ, tWZ.

Vector-boson backgrounds: Z+jets, W+jets, ZZ, ZW, WW.

Event selection (preselection)

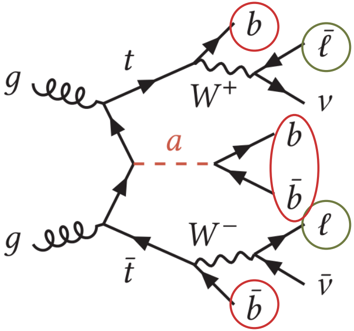

tt $\rightarrow \ell\ell$ selection

- 2 leptons (ee, $\mu\mu$ or $e\mu$).
- One **trigger** lepton with $p_T > 27$ GeV.
- Another lepton with $p_T > 10$ GeV.
- $|m_{\ell\ell} - m_Z| > 8$ GeV.

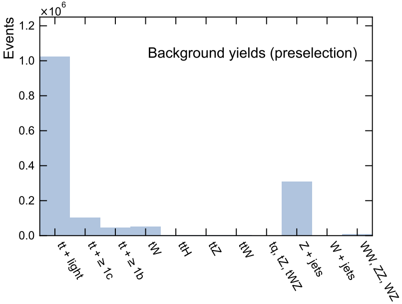

Multi-jet selection

- $N_{\text{jets}} \geq 3$
- $N_{b\,\text{Loose}} \geq 1$

Background modelling

- The main background is $t\bar{t}$+jets.
- Mismodelling observed in both normalisation and shape.
- **Data-driven** reweighting calculated in a **signal-depleted region**.

$t\bar{t}$+jets reweighting region

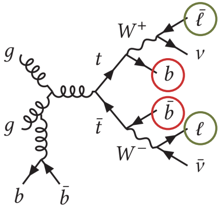

- Preselection
- $e\mu$
- $N_B = 0$
- $N_b \geq 2$

Background modelling

Normalisation of the $t\bar{t}$+light, $t\bar{t}+\geq 1c$ and $t\bar{t}+\geq 1b$ **categories** is corrected using a fit to data over the `sumPCBTag` distribution:

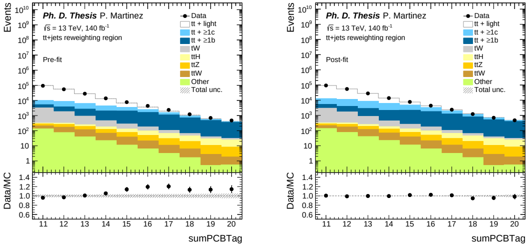

This corrects the N_{jets} distribution as well.

Residual shape mismodelling in the p_T of jets and leptons is corrected using a fit over H_T^{red}:

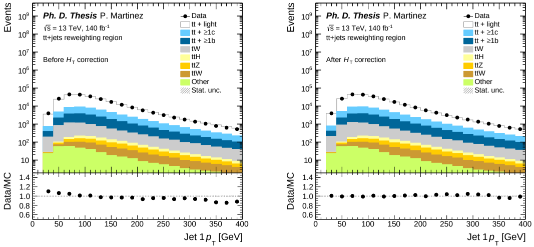

Slides 83 – 85.

BDTs for event reconstruction

BDTs for $t \to j\ell$ reconstruction

- 2 BDTs: **top** and **anti-top** decay.
- Trained with $t\bar{t}$+jets and $t\bar{t}a$ samples.
- Evaluates all permutations between the lepton and the 5 leading jets.

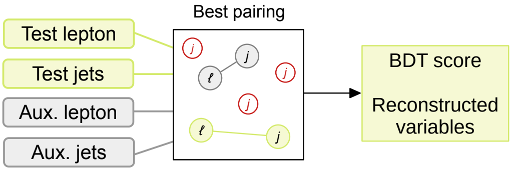

BDT for $a \to jj$ reconstruction

- Trained with $t\bar{t}$+jets and $t\bar{t}a$ samples.
- Evaluates all permutations between the 5 leading jets.

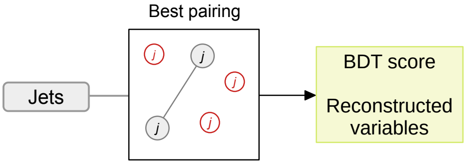

Slides 86 – 88.

NN for signal vs. background discrimination

- 4 training regions:
  - **Boosted:** 1B2b and 1B1b.
  - **Resolved:** 0B4b and 0B3b.
- One training per region (mass-parametrised).

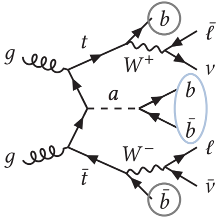

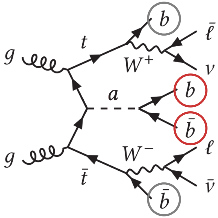

Resonance from $a \to b\bar{b}$

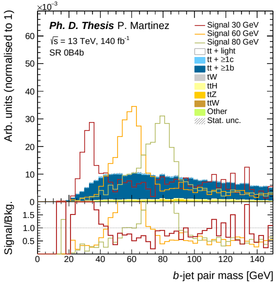

Resonance from $a \to B$

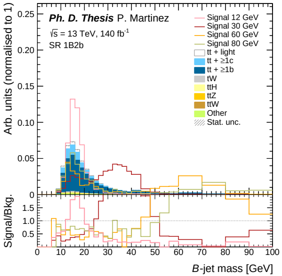

Slides 89 – 91.

Systematic uncertainties

Experimental uncertainties

Detector response, efficiency and calibration. Applied to all signal and background processes.

- Luminosity.
- Pileup modelling.
- Trigger efficiency.
- Object reconstruction and identification (electrons, muons, jets and tracks).
- Flavour tagging.
- $E_{\mathrm{T}}^{\mathrm{miss}}$.

Modelling uncertainties

Theoretical assumptions and limitations in the MC simulation. Applied to signal and the main backgrounds ($t\bar{t}$+jets, tW, $t\bar{t}H$ and $t\bar{t}Z$).

- Renormalisation and factorisation scales (μ_{R}, μ_{F}).
- Parton distribution functions (PDFs).
- Initial and final state radiation (ISR and FSR).
- Alternative hard scattering simulation.
- Alternative parton shower simulation.
- Alternative Monte Carlo parameters.
- Reweighting uncertainties.

Fit setup

Statistical treatment

- One fit per mass hypothesis (10 in total):
  $\boldsymbol{m_a \in [12, 16, 20, 25, 30, \ldots}$
  $\boldsymbol{\ldots 40, 50, 60, 80, 100]}$ **GeV**
- Binned maximum-likelihood fit to the data.

  Free parameters:
  - Signal strength (μ)
  - 3 $t\bar{t}$+jets normalisation factors.
- Systematic uncertainties enter the fit as **nuisance parameters**.
  - Pruning at 1%.

Signal and control regions

- 4 SRs $\Rightarrow$ Fit to the **NN score**.
  - **Boosted**: 1B2b and 1B1b+1bL
  - **Resolved**: 0B4b and 0B3b .
- 1 CR (0B2b+1bL) for the $t\bar{t}$+light and $t\bar{t}$+$\geq$1c categories.

  $\Rightarrow$ Fit to the central bins of the `sumPCBTag` distribution.

Results from the fit to data (m_a = 30 GeV)

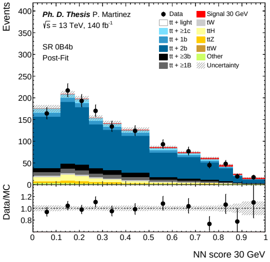

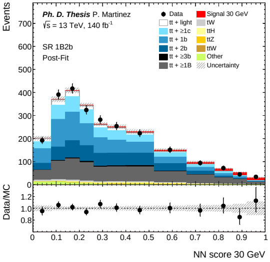

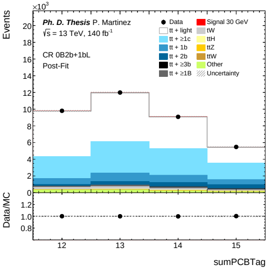

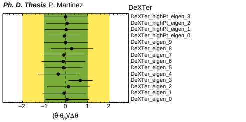

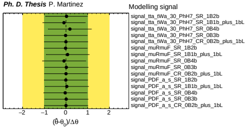

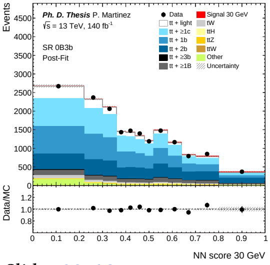

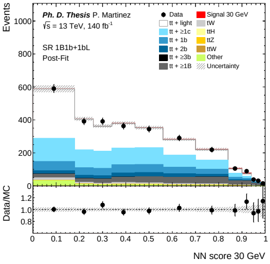

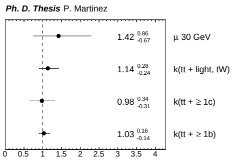

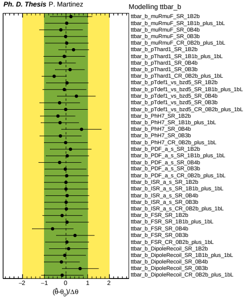

Slides 92, 93.

Exclusion limits

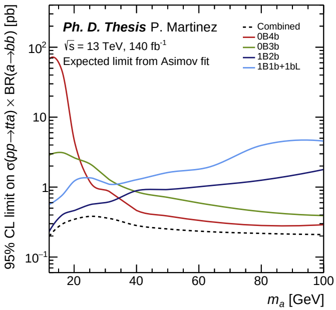

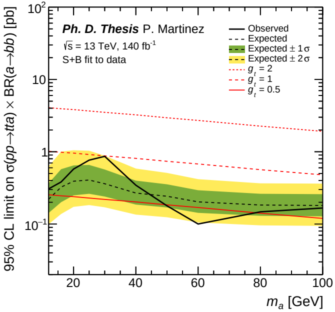

- **No significant excess** above the SM is observed.
- 95% CL limits to $\boldsymbol{\sigma(t\bar{t}a)\times \mathrm{BR}(a\to b\bar{b})}$ **between 0.1 and 0.9 pb** for $\boldsymbol{m_a \in [12, 100]}$ **GeV**.
- The dominant sources of uncertainty are ***B*-tagging** and $\boldsymbol{t\bar{t}+\geq 1b}$ **modelling**.

Category	**Impact on $\hat{\mu}$**
Total stat.	30.0%
Total syst.	49.0%
General	0.8%
Lepton reconstruction	0.1%
Jet reconstruction	10.7%
Track reconstruction	3.2%
$E_{\mathrm{T}}^{\mathrm{miss}}$	0.6%
B-tagging	39.2%
b-tagging	7.8%
Signal modelling	16.4%
$t\bar{t}$+light modelling	4.3%
$t\bar{t}+\geq 1c$ modelling	4.0%
$t\bar{t}+\geq 1b$ modelling	27.7%
tW modelling	1.6%
$t\bar{t}H$ modelling	0.6%
$t\bar{t}Z$ modelling	0.5%
Reweighting	<0.1%
MC stats.	6.6%
Signal MC stats.	6.5%
Norm. factors	14.8%

Summary

→ Two searches for **light spin-0 particles** (a-bosons) are presented.
- They are performed using the full Run 2 dataset (140 fb^{-1} of pp collisions) recorded by the ATLAS experiment.

→ **No significant excesses** over the SM expectation are found.
- Upper limits to $\text{BR}(H \rightarrow aa \rightarrow 4b)$ range between 5% and 25% for $m_a \in [12, 60]$ GeV.
- Upper limits to $\sigma(t\bar{t}a) \times \text{BR}(a \rightarrow b\bar{b})$ range between 0.1 and 0.9 pb for $m_a \in [12, 100]$ GeV.

→ Both searches provide **unprecedented sensitivity**.
- The $H \rightarrow aa \rightarrow 4b$ search uses novel techniques to exploit the characteristics of low-p_{T}, boosted topologies.
- The $t\bar{t}a$, $a \rightarrow b\bar{b}$ search is the first of its kind in both ATLAS and CMS.

→ In addition to Physics data analysis, work has been carried out in the **ATLAS L1Topo trigger simulation** in preparation for Run 3.

Publications

Published:

- P. Martínez Suárez, *The ATLAS Level-1 Topological Processor: experience and upgrade plans*, PoS LHCP2021 (2021) 242 .
- P. Martínez Suárez, *Searches for axion-like-particles (ALPs) in Higgs boson decays in ATLAS*, PoS ICHEP2024 (2024) 071 .
- ATLAS Collaboration, *The ATLAS trigger system for LHC Run 3 and trigger performance in 2022*, JINST 19 P06029 (2024) .

Currently under ATLAS review (to be submitted soon):

- $H \longrightarrow aa \longrightarrow 4b/6b$ in the 0ℓ and 2ℓ channels ($\longrightarrow$ Physical Review D).
- $t\bar{t}a$, $a \longrightarrow b\bar{b}$ ($\longrightarrow$ European Physical Journal C).

Slides 95 – 98.

Thank you for your attention

BACKUP

Theoretical framework

The Brout-Englert-Higgs mechanism

$$\Phi = \frac{1}{\sqrt{2}}\begin{pmatrix}\phi^+ \\ \phi^0\end{pmatrix}$$

$$\Phi(x) = \frac{1}{\sqrt{2}} e^{i\boldsymbol{T}\cdot\boldsymbol{\xi}(x)/v}\begin{pmatrix}0 \\ v + H(x)\end{pmatrix} \approx \frac{1}{\sqrt{2}}\begin{pmatrix}\frac{1}{2}(\xi_2 + i\xi_2) \\ v + H - \frac{1}{2}i\xi_3\end{pmatrix}$$

$$\begin{aligned}\mathcal{L}_{\mathrm{SSB}} &= (D_\mu\Phi)^\dagger(D^\mu\Phi) - V(\Phi) \\ &= (D_\mu\Phi)^\dagger(D^\mu\Phi) - \left[\mu^2(\Phi^\dagger\Phi) + \lambda(\Phi^\dagger\Phi)^2\right]\end{aligned}$$

$$\begin{aligned}W_\mu^\pm &= \frac{1}{\sqrt{2}}(W_\mu^1 \mp iW_\mu^2), \\ A_\mu &= B_\mu \cos\theta_W + W_\mu^3 \sin\theta_W, \\ Z_\mu &= -B_\mu \sin\theta_W + W_\mu^3 \cos\theta_W\end{aligned}$$

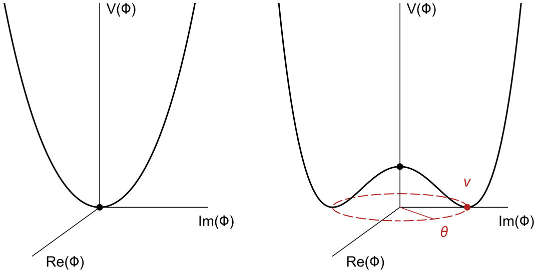

$$g \sin\theta_W = g' \cos\theta_W = e$$

2 Higgs doublet model (2HDM)

$$V_{\text{2HDM}}(\Phi_1,\Phi_2) = \mu_1^2\Phi_1^\dagger\Phi_1 + \mu_2^2\Phi_2^\dagger\Phi_2 - \mu_3^2(\Phi_1^\dagger\Phi_2 + \text{h.c.}) + \frac{1}{2}\lambda_1(\Phi_1^\dagger\Phi_1)^2 + \frac{1}{2}\lambda_2(\Phi_2^\dagger\Phi_2)^2 + \lambda_3(\Phi_1^\dagger\Phi_1)(\Phi_2^\dagger\Phi_2) + \lambda_4(\Phi_1^\dagger\Phi_2)(\Phi_2^\dagger\Phi_1) + \frac{1}{2}\lambda_5\left[(\Phi_1^\dagger\Phi_2)^2 + \text{h.c.}\right],$$

$$V_P = \frac{1}{2}m_P^2P^2 + P(ib_P\Phi_1^\dagger\Phi_2 + \text{h.c.}) + P^2(\lambda_{P,1}\Phi_1^\dagger\Phi_1 + \lambda_{P,2}\Phi_2^\dagger\Phi_2)$$

Parameter	Value
$\tan\beta$	1
$\sin\theta$	0.7
λ_3	3
$\lambda_{P,1}$	3
$\lambda_{P,2}$	3
y_χ	1

Table 3.4: 2HDM+a parameters used in the $t\bar{t}a$, $a \to b\bar{b}$ analysis.

Coupling	Type I	Type II	Type III	Type IV
$\xi_{h,\ell}$	1	1	1	1
$\xi_{h,u}$	1	1	1	1
$\xi_{h,d}$	1	1	1	1
$\xi_{H,\ell}$	$-\cot\beta$	$\tan\beta$	$\tan\beta$	$-\cot\beta$
$\xi_{H,u}$	$-\cot\beta$	$-\cot\beta$	$-\cot\beta$	$-\cot\beta$
$\xi_{H,d}$	$-\cot\beta$	$\tan\beta$	$-\cot\beta$	$\tan\beta$
$\xi_{A,\ell}$	$-\cot\beta$	$\tan\beta$	$\tan\beta$	$-\cot\beta$
$\xi_{A,u}$	$\cot\beta$	$\cot\beta$	$\cot\beta$	$\cot\beta$
$\xi_{A,d}$	$-\cot\beta$	$\tan\beta$	$-\cot\beta$	$\tan\beta$

Table 3.3: Yukawa coupling strength for the neutral h, H and A in the four 2HDM models at the decoupling limit $\alpha \to \beta - \pi/2$. The notation $\ell = e, \mu, \tau$, $u = u, c, t$ and $d = d, s, b$ is used.

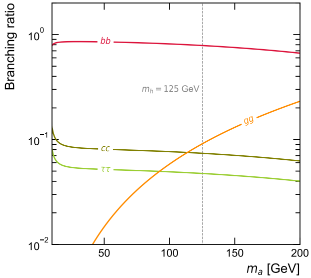

Higgs boson properties

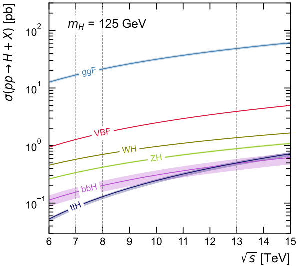

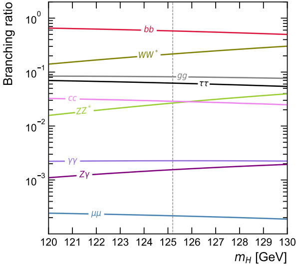

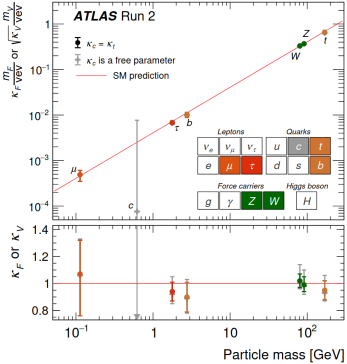

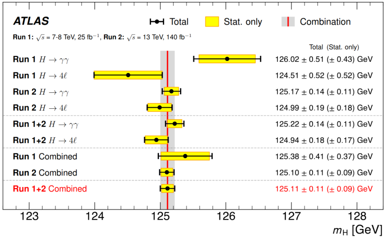

Standard Model cross section measurements

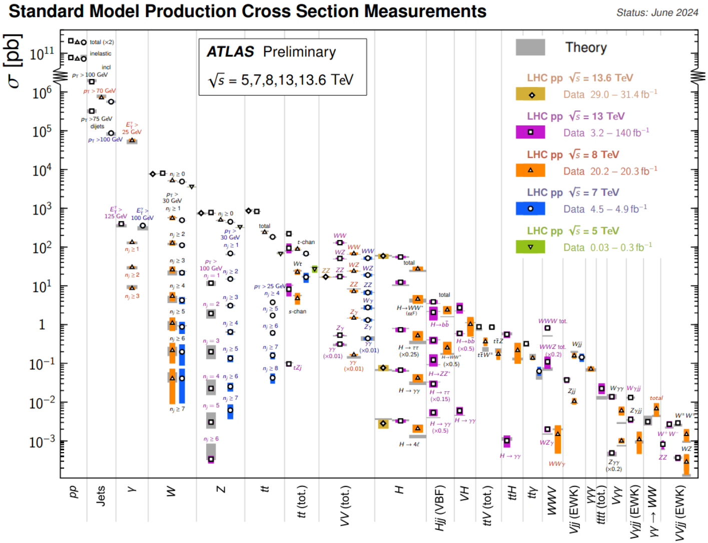

Experimental setup

ATLAS ID schematics

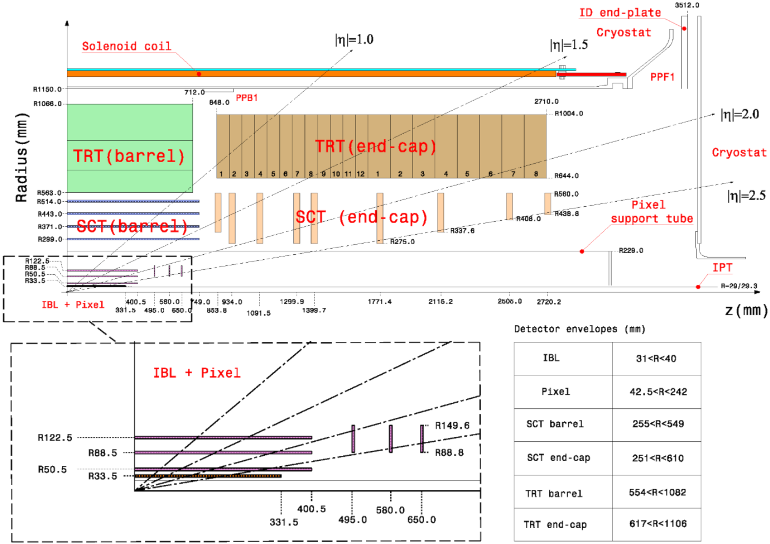

Detector envelopes (mm)

IBL	31<R<40
Pixel	42.5<R<242
SCT barrel	255<R<549
SCT end-cap	251<R<610
TRT barrel	554<R<1082
TRT end-cap	617<R<1106

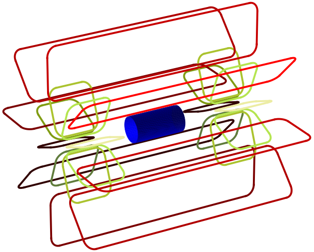

ATLAS calorimeter schematics

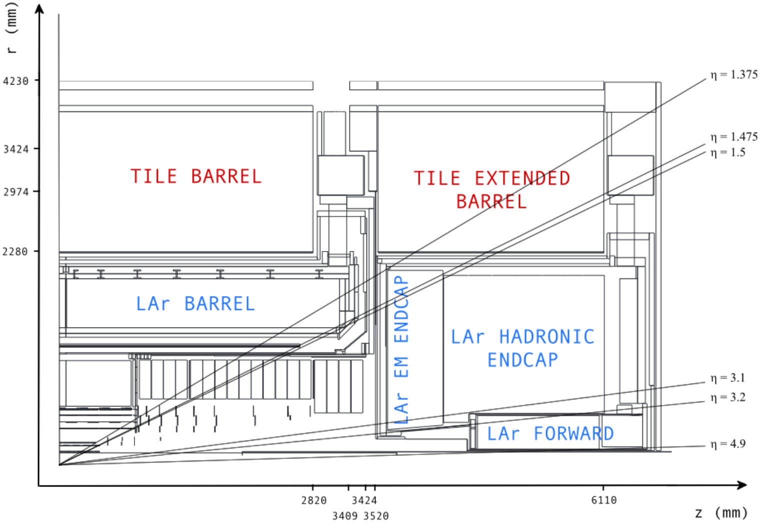

Jet reconstruction

$$d_{ij} = \min\left(p_{\mathrm{T},i}^{2p}, p_{\mathrm{T},j}^{2p}\right)\frac{\Delta_{ij}^2}{R}$$
$$d_{iB} = p_{\mathrm{T},i}^{2p}$$

If $d_{ij} < d_{iB} \longrightarrow$ cluster.
Else $\longrightarrow i =$ final jet.

Inclusive clustering: end when all particles are part of a jet with $R_{ij} > R \; \forall \; i, j$.
Exclusive clustering: end when the desired amount of jets is found.

$\boldsymbol{p = 1}$: k_T algorithm.
$\boldsymbol{p = -1}$: anti-k_T algorithm.
$\boldsymbol{p = 0}$: Cambridge/Aachen algorithm.

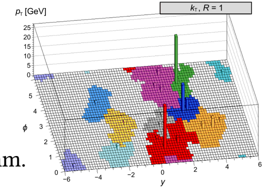

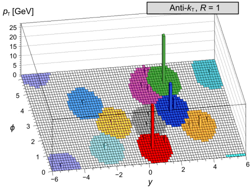

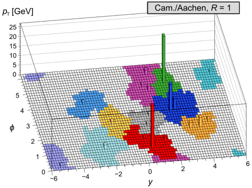

ATLAS MS schematics

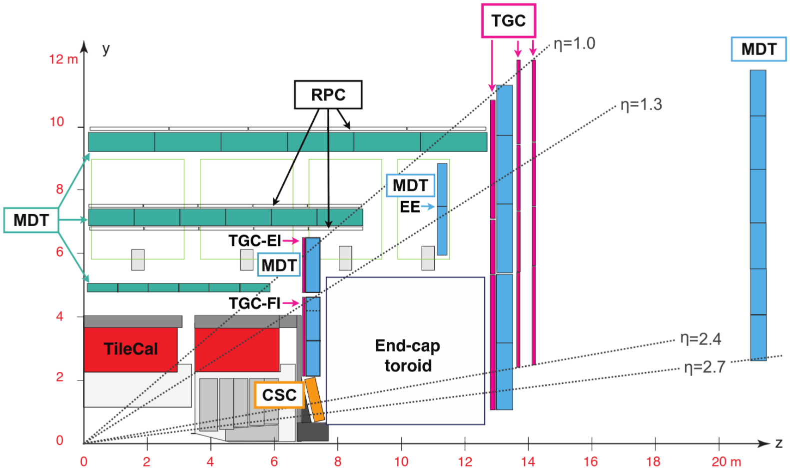

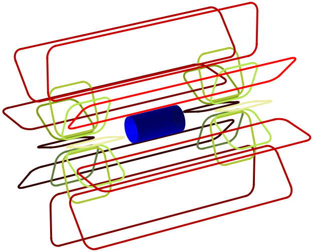

ATLAS TDAQ – Run 2 layout

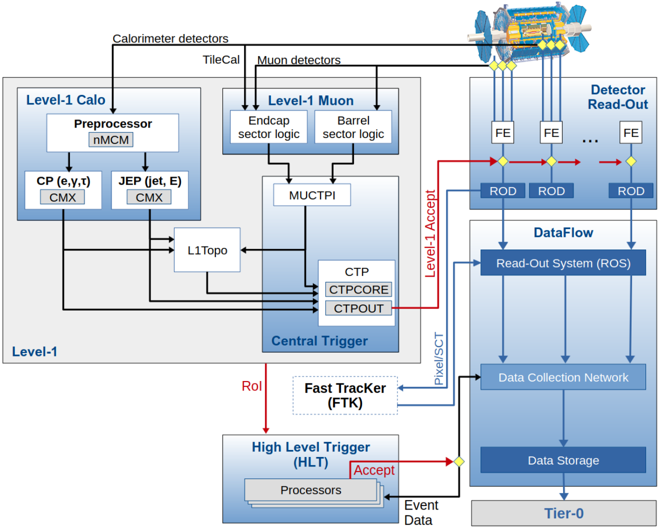

L1Topo Run 2

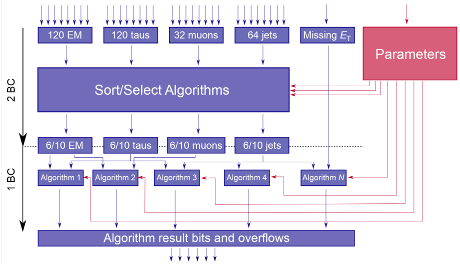

L1Topo algorithm	Definition
Pseudorapidity distance	$\Delta\eta_{min} \leq \Delta\eta = \lvert\eta_1 - \eta_2\rvert \leq \Delta\eta_{max}$
Azimuthal distance	$\Delta\phi_{min} \leq \Delta\phi = \lvert\phi_1 - \phi_2\rvert \leq \Delta\phi_{max}$
Box cut	$\Delta\eta_{min} \leq \Delta\eta \leq \Delta\eta_{max}$ and $\Delta\phi_{min} \leq \Delta\phi \leq \Delta\phi_{max}$
Window cut	$\eta_{min} < \eta < \eta_{max}$ and $\phi_{min} < \phi < \phi_{max}$
Angular distance	$\Delta R^2_{min} \geq \Delta R^2 = \Delta\eta^2 + \Delta\phi^2 \leq \Delta R^2_{max}$
Disambiguation	$\eta_1 \neq \eta_2$ or $\phi_1 \neq \phi_2$ or $\Delta R > \Delta R_{min}$
Ratio	$f(\mathrm{TOB}_1) \geq \alpha f(\mathrm{TOB}_2)$ with $\eta_1 = \eta_2, \phi_1 = \phi_2$ and α = constant
Invariant mass	$m^2_{\mathrm{inv,min}} \leq m^2_{\mathrm{inv}} = 2E^1_{\mathrm{T}}E^2_{\mathrm{T}}(\cosh\Delta\eta - \cos\Delta\phi) \leq m^2_{\mathrm{inv,max}}$
Transverse mass	$m^2_{\mathrm{T,min}} \leq m^2_{\mathrm{T}} = 2E^1_{\mathrm{T}}E^{\mathrm{miss}}_{\mathrm{T}}(1 - \cos\Delta\phi) \leq m^2_{\mathrm{T,max}}$
Event hardness	$H_{\mathrm{T,min}} < H_{\mathrm{T}} = \sum p^{\mathrm{jets}}_{\mathrm{T}}$
Simple cone	$E_{\mathrm{T,min}} < E^{\mathrm{cone}}_{\mathrm{T}} = \sum_{\Delta R<1.0} E^{\mathrm{jets}}_{\mathrm{T}}$
Late muon	Finds the highest-p_{T} μ in the next BC and combines it with the input lists associated with the current BC.

Physics simulation

Hard scattering

$$\sigma_{pp\to X} = \sum_{i,j} \int_0^1 dx_1 dx_2 \; f_i(x_1,\mu_F^2) f_j(x_2,\mu_F^2) \hat{\sigma}_{ij\to X}\left(x_1P_1, x_2P_2, \frac{Q^2}{\mu_F^2}, \frac{Q^2}{\mu_R^2}\right)$$

PDFs

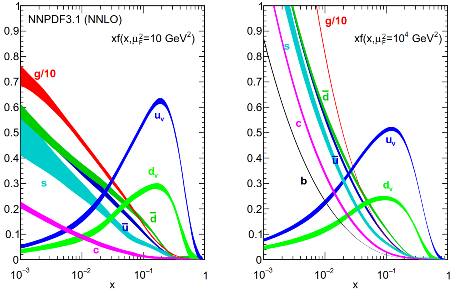

DGLAP and Parton Shower

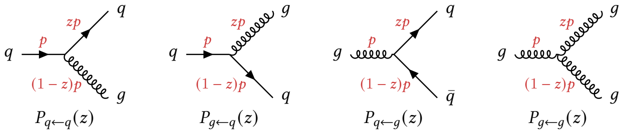

$$d\sigma \approx \sigma_{\mathrm{ME}} \sum_i \frac{\alpha_s}{2\pi}\frac{d\theta^2}{\theta^2} dz P_{j\leftarrow i}(z)$$

$$\Lambda_i(t_{\max}^2, t^2) = \exp\left[\int_{t^2}^{t_{\max}^2} \frac{\alpha_s}{2\pi}\frac{d\tilde{t}^2}{\tilde{t}^2}\int_{t_0^2/\tilde{t}^2}^{1-t_0^2/\tilde{t}^2} dz P_{j\leftarrow i}(z)\right]$$

Search for decays of the Higgs boson into pseudoscalar particles decaying to four bottom quarks using proton-proton collisions at $\sqrt{s} = 13$ TeV with the ATLAS detector

DL1r b-tagging

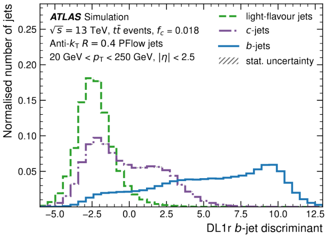

$$D_{\mathtt{DL1r}} = \ln\left(\frac{p_b}{f_c p_c + (1 - f_c) p_l}\right)$$

DL1r ε_b	DL1r WP	b-tagging score
100-85%	None	1
85-77%	85	2
77-70%	77	3
70-60%	70	4
60-0%	60	5

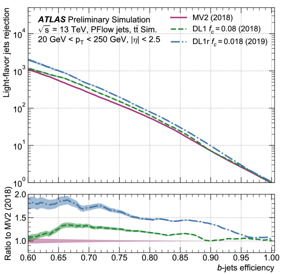

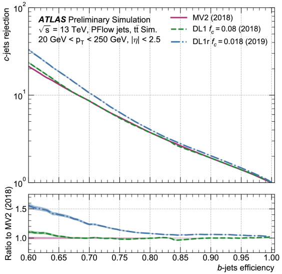

DeXTer B-tagging

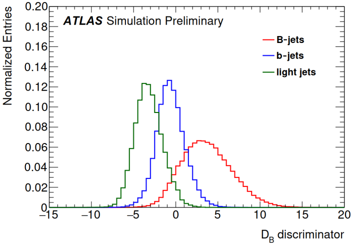

$$D_{\mathtt{DeXTer}} = \ln\left(\frac{p_B}{(1-f_b)p_l + f_b p_b}\right)$$

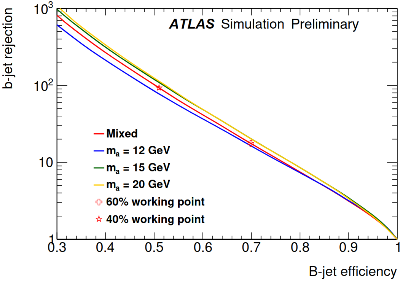

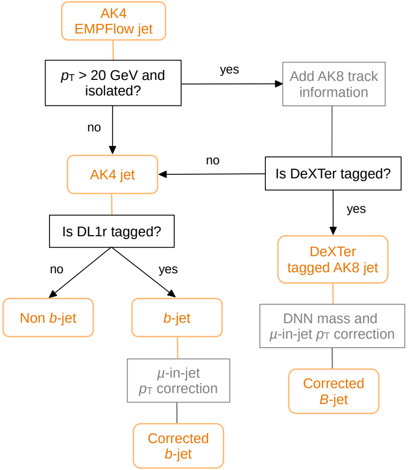

TC-LVT SV-tagging

$p_{\mathrm{T}} > 3$ GeV
$m_v > 600$ MeV

$H \rightarrow aa \rightarrow 4b$ truth plots

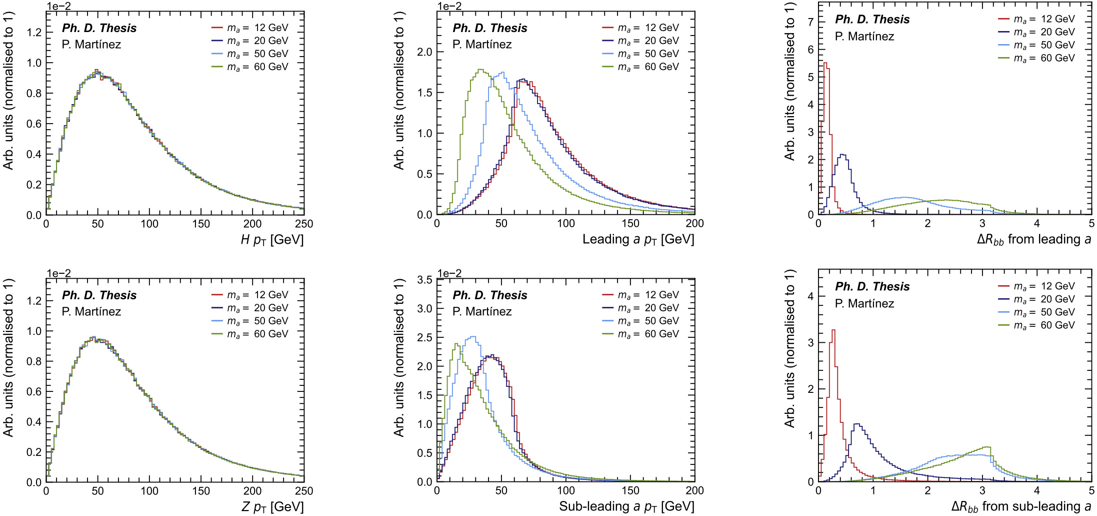

Background modelling

tt+jets (left) and Z+jets (right) fit to H_T^{red}

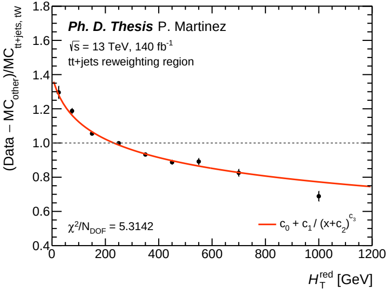

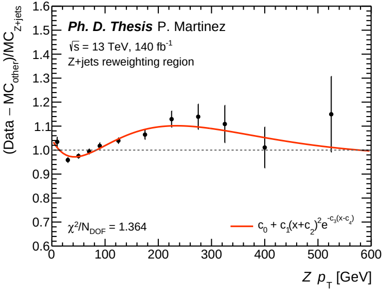

Background modelling

tt+jets H_T correction – before and after

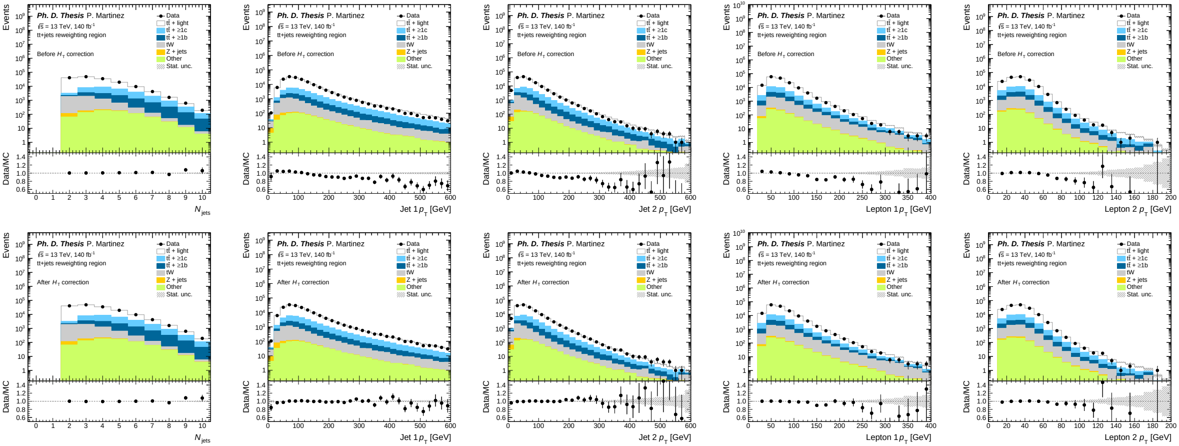

Background modelling

Z+jets p_T correction – before and after

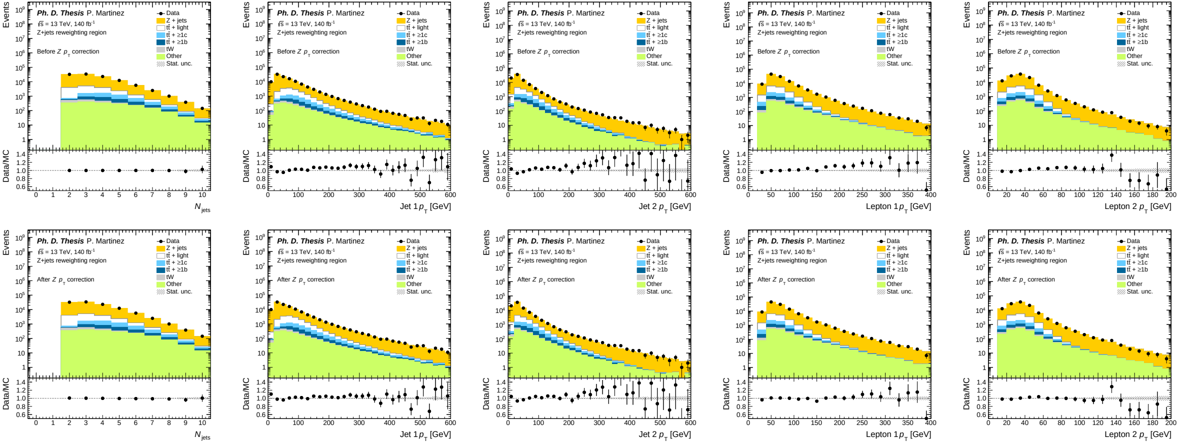

NN for event reconstruction

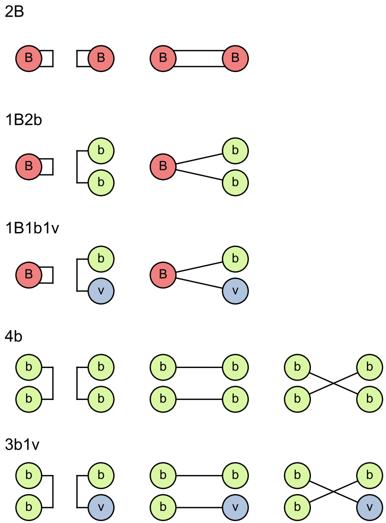

Object	Feature	Description
Ak8 jets	$\log m$	DNN-corrected track jet mass
	$\log p_{\mathrm{T}}$	Transverse momentum
	η	Pseudorapidity
	ϕ	Azimuthal angle
	`isDeXTer60WP`	True if the jet is `DeXTer` tagged with 60% WP
	`isDeXTer40WP`	True if the jet is `DeXTer` tagged with 40% WP
Ak4 jets	$\log m$	Invariant mass
	$\log p_{\mathrm{T}}$	Transverse momentum
	η	Pseudorapidity
	ϕ	Azimuthal angle
	`DL1r` b-tagging score	PC `DL1r` tagging score
Soft v	$\log m$	Track mass
	$\log p_{\mathrm{T}}$	Transverse momentum
	η	Pseudorapidity
	ϕ	Azimuthal angle
	$L_{3\mathrm{D}}$	Decay length relative to the primary vertex
	$S_{L_{3\mathrm{D}}}$	Decay length significance
Z boson candidate (ee or $\mu\mu$)	p_{T}	Transverse momentum
	η	Pseudorapidity
	ϕ	Azimuthal angle
	m	Invariant mass

BDT for signal vs. background discrimination – Example inputs

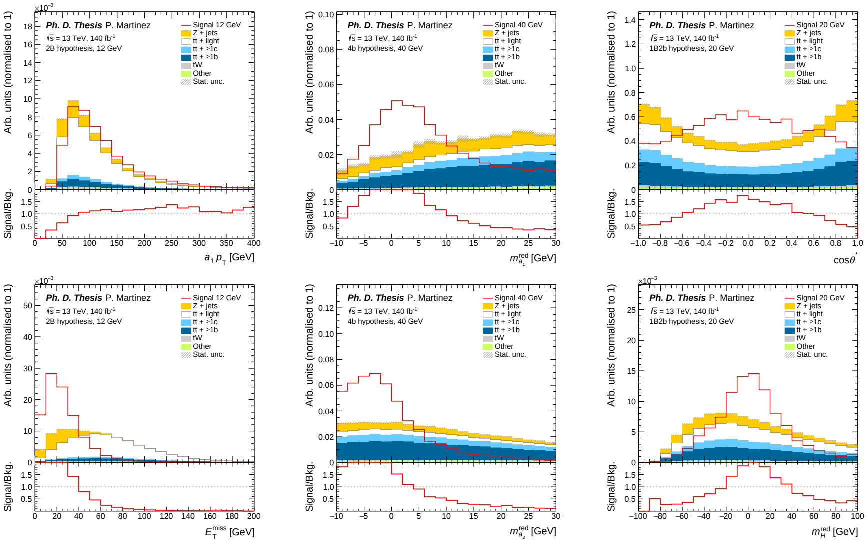

SR and CR composition

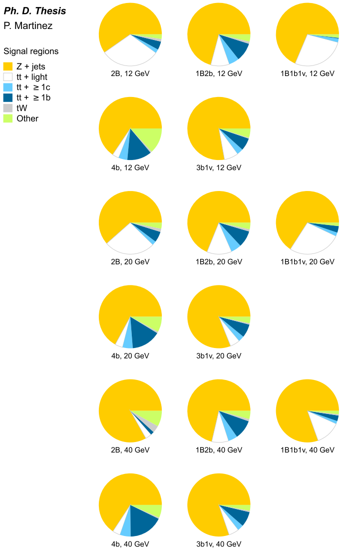

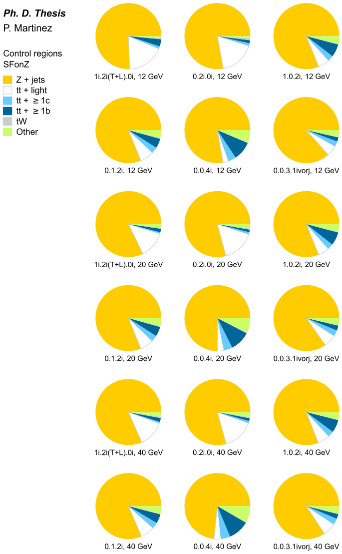

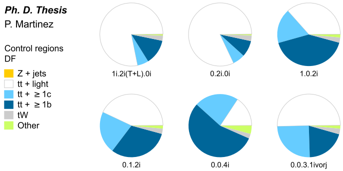

Results from the fit to data (m_a = 25 GeV)

Correlation matrix and ranked systematics

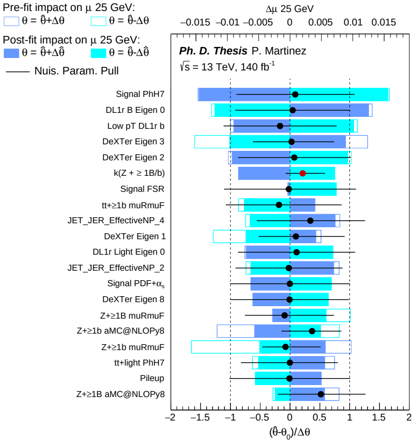

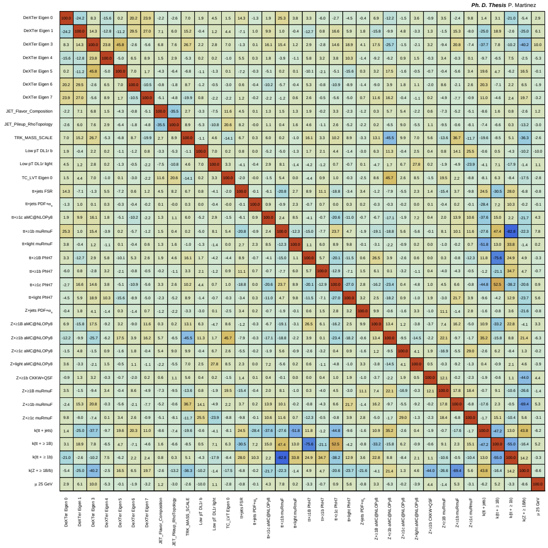

Results from the fit to data (m_a = 25 GeV)

Relevant systematic variations in the signal and control regions

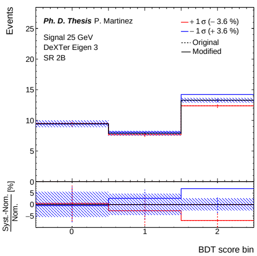

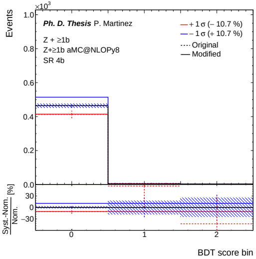

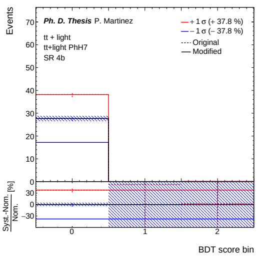

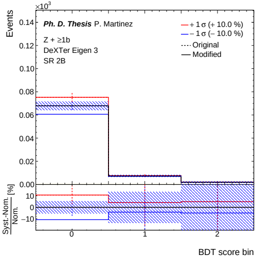

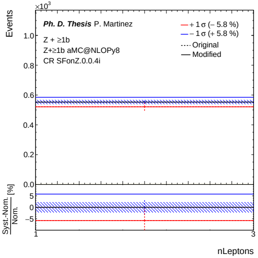

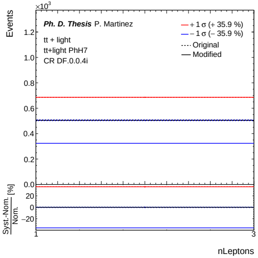

Result comparison

Comparison with other $H \rightarrow aa$ final states (left) and equivalent CMS analyses (right)

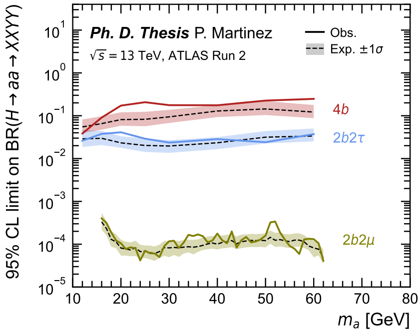

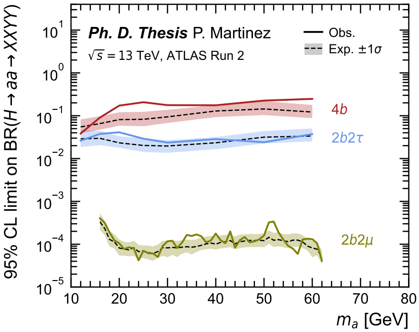

Search for a new pseudoscalar decaying into a pair of bottom and anti-bottom quarks in top-associated production using proton-proton collisions at $\sqrt{s} = 13$ TeV with the ATLAS detector

tta, $a \rightarrow bb$ truth plots

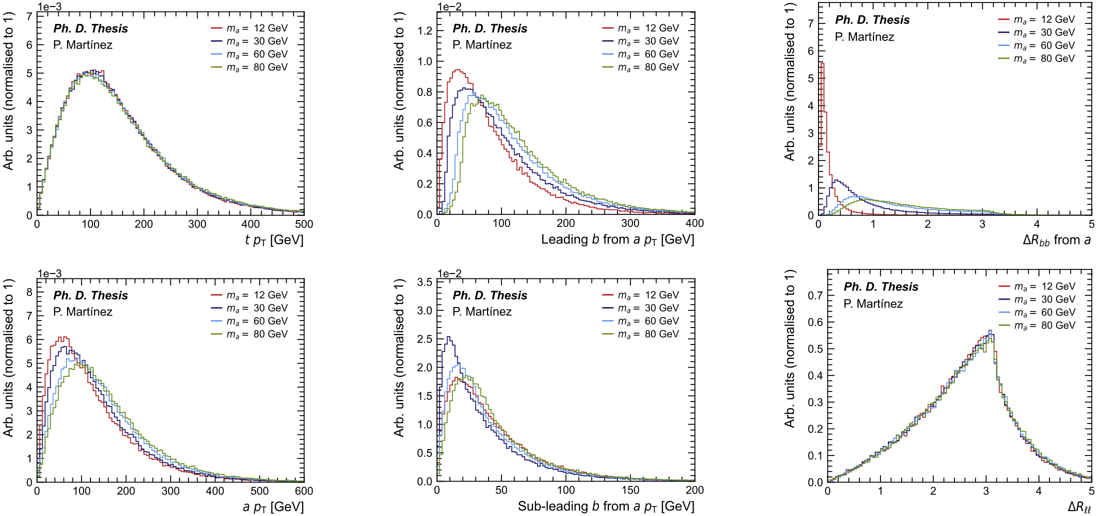

tta vs. *tWa* cross section

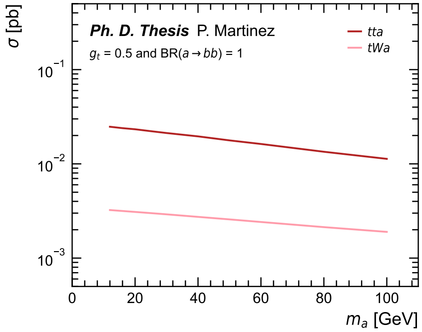

Background modelling

$t\bar{t}$+jets norm. correction – effect on the N_{jets} distribution

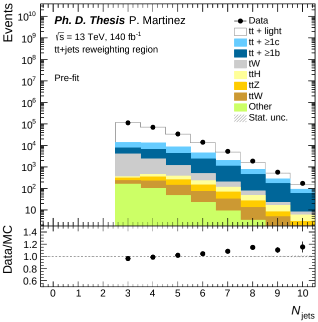

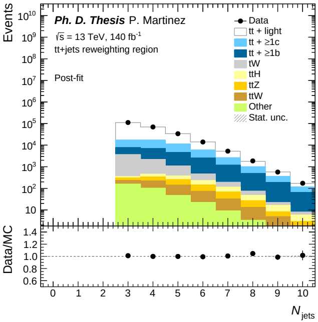

Background modelling

tt+jets fit to H_T^{red}

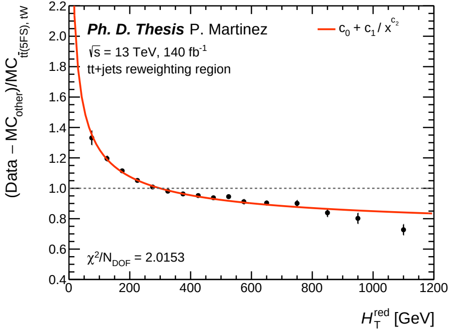

Background modelling

$t\bar{t}$+jets H_T correction – before and after

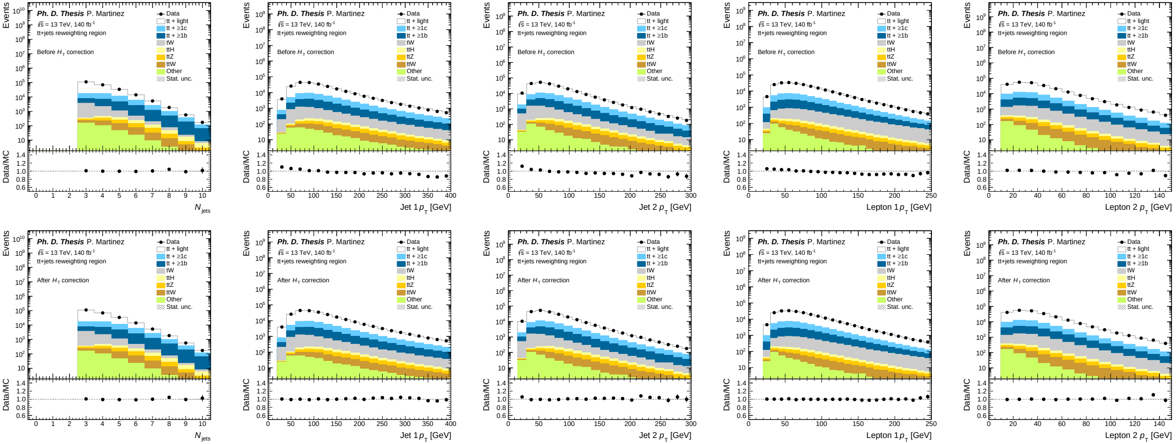

BDTs for event reconstruction

Sample	Events
$t\bar{t}a$ 12 GeV	30000
$t\bar{t}a$ 16 GeV	30000
$t\bar{t}a$ 20 GeV	30000
$t\bar{t}a$ 30 GeV	30000
$t\bar{t}a$ 40 GeV	30000
$t\bar{t}a$ 60 GeV	30000
$t\bar{t}a$ 80 GeV	30000
$t\bar{t}a$ 100 GeV	30000
$t\bar{t}$+jets	30000
$t\bar{t}$+jets `BBFilt`	30000
$t\bar{t}$+jets `BFiltBBVeto`	30000
$t\bar{t}$+jets `CFiltBVeto`	30000

Table 11.8: Number of $t\bar{t}a$ and $t\bar{t}$+jets MC events used in the training of the $t \rightarrow j\ell$ reconstruction BDTs.

Object	Variables
Full event	N_{jets}, $N_{b\text{-jets}}$ (85% WP)
Test/aux. $j\ell$ pair	m, p_{T}, η, ΔR
Test/aux. jet	p_{T}, η, b-tagging score, jet ID
Test/aux. lepton	p_{T}, η
$t\bar{t}$ pair	m, p_{T}, η, ΔR, $\Delta\phi$
jj pair	ΔR

Table 11.9: Input variables to the $t \rightarrow j\ell$ reconstruction BDTs. Kinematic variables of the $t\bar{t}$ pair are computed using $j\ell$ and $j\bar{\ell}$.

Sample	Events
$t\bar{t}a$ 12 GeV	106067
$t\bar{t}a$ 16 GeV	103016
$t\bar{t}a$ 20 GeV	107246
$t\bar{t}a$ 30 GeV	110104
$t\bar{t}a$ 40 GeV	112470
$t\bar{t}a$ 60 GeV	114470
$t\bar{t}a$ 80 GeV	115680
$t\bar{t}a$ 100 GeV	116434
$t\bar{t}$+jets	120000
$t\bar{t}$+jets `BBFilt`	120000
$t\bar{t}$+jets `BFiltBBVeto`	120000
$t\bar{t}$+jets `CFiltBVeto`	120000

Table 11.10: Number of $t\bar{t}a$ and $t\bar{t}$+jets MC events used in the training of the $a \rightarrow jj$ reconstruction BDT.

Object	Variables
Full event	N_{jets}, $N_{b\text{-jets}}$ (85% WP), `sumPCBTag`
jj pair	m, p_{T}, η, E, ϕ, ΔR
Test jet 1	p_{T}, η, b-tagging score, jet ID
Test jet 2	p_{T}, η, b-tagging score, jet ID

Table 11.11: Input variables to the $a \rightarrow jj$ reconstruction BDT.

Outputs from the $t \to j\ell$ BDT – Examples

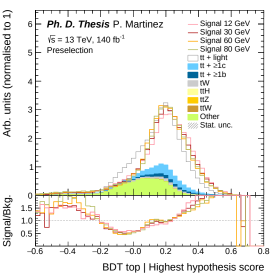

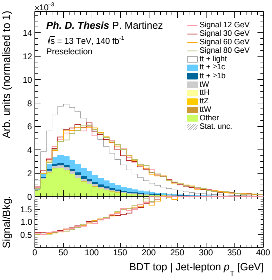

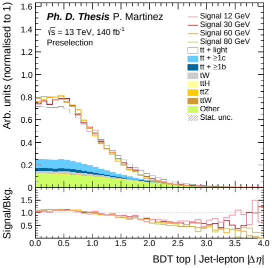

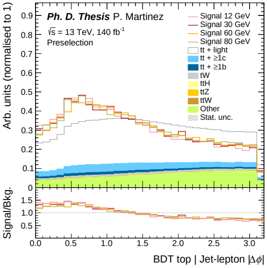

Outputs from the $a \to jj$ BDT – Examples

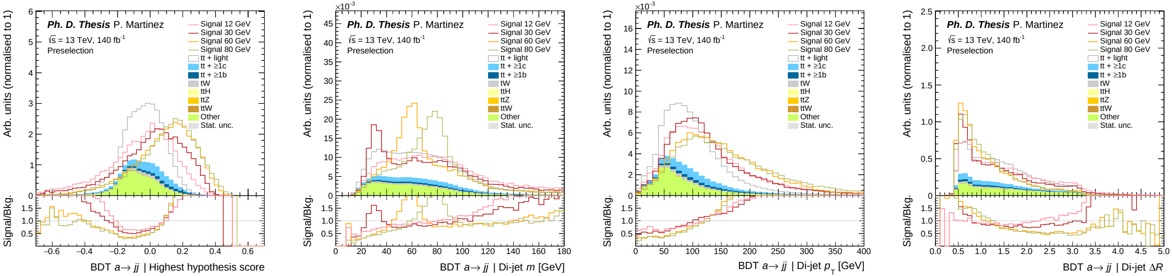

NN for signal vs. background discrimination

Sample	0B4b	0B3b	1B2b	1B1b
$t\bar{t}a$ 12 GeV	–	15353	11096	16269
$t\bar{t}a$ 16 GeV	–	13669	11028	15878
$t\bar{t}a$ 20 GeV	1045	15440	10148	14896
$t\bar{t}a$ 30 GeV	3447	20801	7239	9964
$t\bar{t}a$ 40 GeV	5721	25618	5157	6891
$t\bar{t}a$ 60 GeV	8624	30650	3604	3803
$t\bar{t}a$ 80 GeV	10087	33083	3261	2925
$t\bar{t}a$ 100 GeV	10973	33916	3310	2685
$t\bar{t}$+light	96	34149	2438	352628
$t\bar{t}+\geq 1c$	1412	122056	6643	48749
$t\bar{t}+\geq 1b$	49703	446433	61772	78655
tW	175	2857	280	3867
Other	195973	715973	71470	141348

Table 11.13: Number of signal and background MC events used in the training of the signal versus background discriminator for each training region. In this table, "Other" includes the $t\bar{t}H$, $t\bar{t}Z$, $t\bar{t}W$, tq, tZ, tWZ, Z/W+jets and diboson background processes. The 12 and 16 GeV $t\bar{t}a$ samples are excluded from the 0B4b training due to low statistics.

Hyperparameter	Value
Hidden layers	2
Hidden size	$2 \times N_{\text{features}}$
Activation function	ReLu
Learning rate	10^{-4}
Epochs	500
Patience	4
Dropout	0.3

Table 11.14: List of hyperparameters used in the NN training. The number of epochs corresponds to the maximum number allowed. The training is stopped if the loss does not improve after 4 epochs (patience). The choice of the values is based on the NN performance and the total training time.

Object	Variables
BDT $t \to j\ell$	Score, $p_T^{j\ell}$, $\Delta R_{j\ell}$, $\Delta\eta_{j\ell}$, $\Delta\phi_{j\ell}$, jet ID
BDT $a \to jj$	Score, p_T^{jj}, η_{jj}, m_{jj}, ΔR_{jj}, $\Delta\eta_{jj}$, $\Delta\phi_{jj}$, jet ID
Small-R jets	p_T, η, b-tagging score p_T^{bb}, m_{bb}, m_{bbb}, m_{bbbb}, ΔR_{bb}, $\Delta\eta_{bb}$, $\Delta\phi_{bb}$, $\Delta\phi_{E_T^{\text{miss}},b}$
Large-R jets	p_T, η, m ΔR_{Bb}, $\Delta\phi_{E_T^{\text{miss}},B}$
Leptons	$\Delta R_{\ell\ell}$, $\Delta\eta_{\ell\ell}$, $\Delta\phi_{\ell\ell}$, $\Delta\phi_{E_T^{\text{miss}},\ell}$ $\Delta R_{\ell\ell,bb}$, $\Delta R_{\ell\ell,B}$, $\Delta R_{\ell\ell,b}$
Event	N_{jets}, H_T^{jets}, E_T^{miss}

Table 11.15: NN input variables. For bb variables, both the pair with maximum p_T and minimum ΔR are included. Angular variables with one b and/or one B use the minimum ΔR pair. m_{bbbb} and m_{bbb} correspond to the combination with maximum p_T.

NN for signal vs. background discrimination – Example inputs

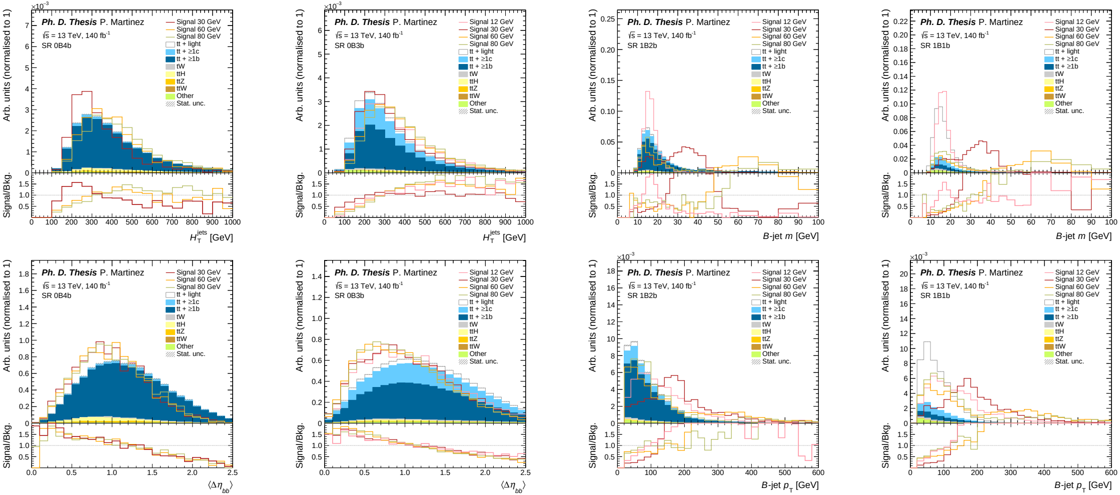

NN for signal vs. background discrimination – AUC per region

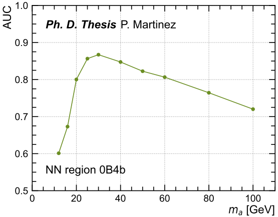

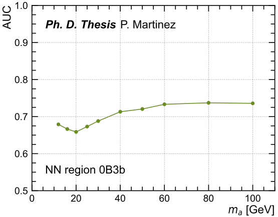

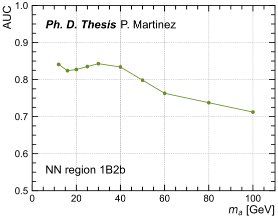

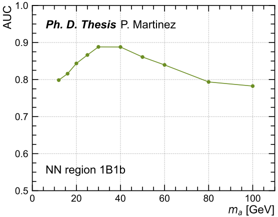

Results from the fit to data (m_a = 30 GeV)

Correlation matrix and ranked systematics

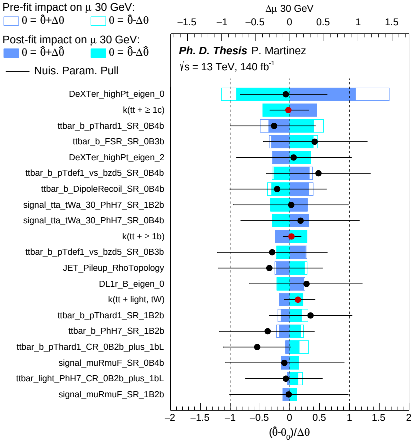

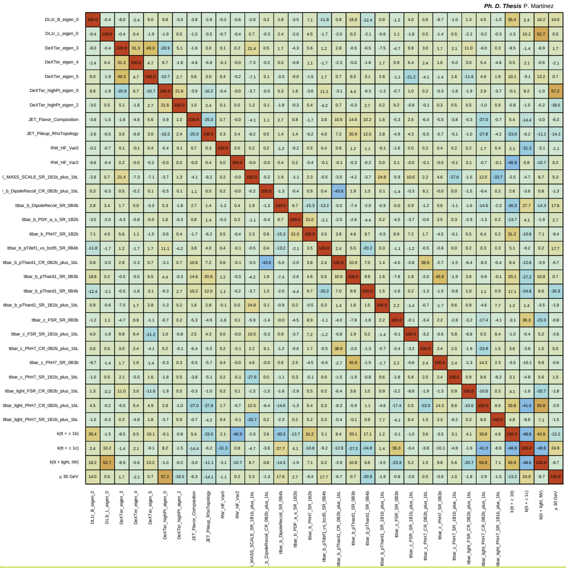

Results from the fit to data (m_a = 30 GeV)

Relevant systematic variations in the signal and control regions

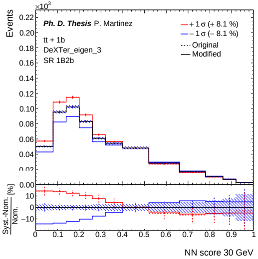

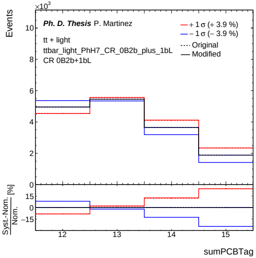

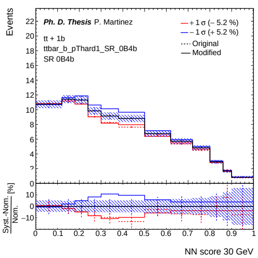

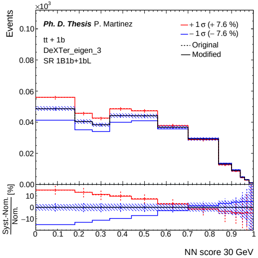

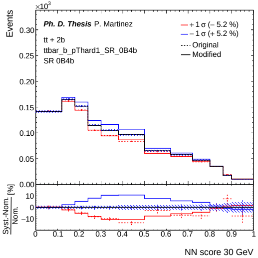

Qualification task

ATLAS TDAQ – Run 3 layout

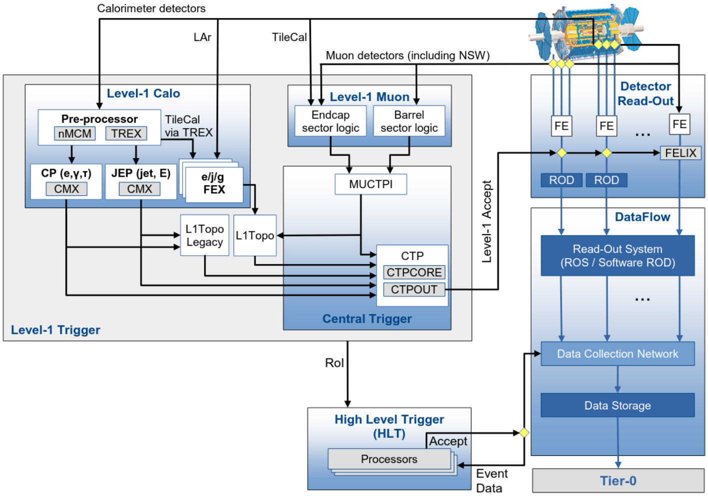

ATLAS MS – Run 3 layout

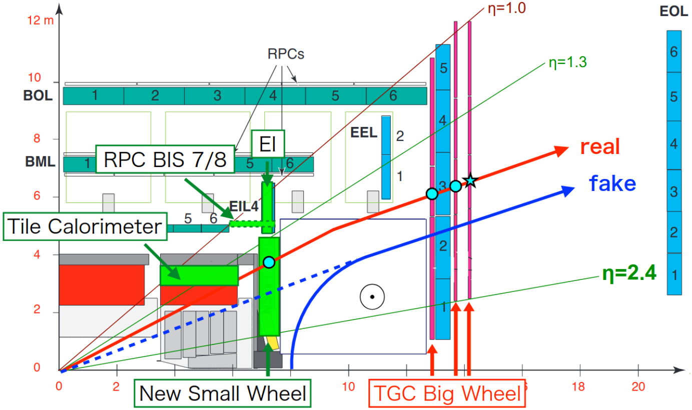

L1Topo TOBs – Run 2 vs. Run 3 (I)

Run 2 TOBs

Name	Description	ΔE_T [GeV]	$\Delta\eta$	$\Delta\phi$
EM Tau	e/γ from CP τ from CP	0.5	0.1	0.1
Jet	Jet from JEP	1	0.2	0.2
MET	Missing transverse energy from JEP	1	–	0.1
Muon	Muon from MUCTPI	RPC p_T thresholds {4, 6, 10, 11, 20, 21} TGC p_T thresholds {4, 6, 10, 15, 20}	0.2-0.4	0.1

Run 3 TOBs

Name	Description	ΔE_T [GeV]	$\Delta\eta$	$\Delta\phi$
eEM eTau	e/γ from eFEX τ from eFEX	0.1	0.025	0.1
jEM jTau jJet jLJet	e/γ from jFEX τ from jFEX Jet from jFEX Large-R jet from jFEX	0.2	0.1	0.1
jXE jTE	Missing transverse energy from jFEX Total transverse energy from jFEX	0.2	–	0.05
gJet gLJet	Jet from gFEX Large-R jet from gFEX	0.2	0.2	0.2
gXE gTE	Missing transverse energy from gFEX Total transverse energy from gFEX	0.2	–	0.2
Muon	Muon from MUCTPI	RPC p_T thresholds {4, 6, 10, 11, 20, 21} TGC p_T thresholds {3, 4, 5, 6, 7, 8, 9, 10, 11 12, 13, 14, 15, 18, 20}	0.025	0.05

L1Topo TOBs – Run 2 vs. Run 3 (II)

Run 2 max. TOBs per event	
EM	120
Tau	120
Jet	64
MET	1
Muon	32

Run 3 max. TOBs per event	
eEM	144
eTau	144
jEM	5
jTau	6
jJet	168
jLJet	24
jXE	7
jTE	7
gJet	6
gLJet	3
gXE	3
gTE	1
Muon	32